NASA TECHNICAL NOTE

NASA TN D-4490

C. 1

NASA TN D-4490

SIMPLE PROCESSORS OF STAR TRACKER COMMANDS FOR STABILIZING AN INERTIALLY ORIENTED SATELLITE

by Robert D. Showman, Brian F. Doolin, and G. Michael Sullivan

Ames Research Center
Moffett Field, Calif.

NATIONAL AERONAUTICS AND SPACE ADMINISTRATION • WASHINGTON, D. C. • MARCH 1968

SIMPLE PROCESSORS OF STAR TRACKER COMMANDS FOR STABILIZING AN INERTIALLY ORIENTED SATELLITE

By Robert D. Showman, Brian F. Doolin,
and G. Michael Sullivan

Ames Research Center
Moffett Field, Calif.

NATIONAL AERONAUTICS AND SPACE ADMINISTRATION

For sale by the Clearinghouse for Federal Scientific and Technical Information
Springfield, Virginia 22151 – CFSTI price $3.00

TABLE OF CONTENTS

TABLE OF CONTENTS - Concluded

SIMPLE PROCESSORS OF STAR TRACKER COMMANDS FOR STABILIZING AN INERTIALLY ORIENTED SATELLITE

By Robert D. Showman, Brian F. Doolin,
and G. Michael Sullivan

Ames Research Center

SUMMARY

The study develops processors which convert star tracker gimbal angle measurements to satellite attitude control signals. An exact processor is nonlinear and complex because the gimbal angles vary as the inertial orientation of the vehicle changes. In this paper, approximations to the exact processor are developed which greatly simplify the mechanization and yet allow satisfactory attitude control.

The approximate processors are derived from a perturbation analysis in which only the first-order terms are considered significant. The first processor, called the ideal processor, is a direct mechanization of the first-order approximation to the exact equations and is the most complex to mechanize. It requires resolvers on the trackers' outer gimbal axes and the computation of the tangent and the sine and cosine of the difference of two angles. Two approximations to the ideal processor, called the partial processor and the constant processor, require less mechanization. The partial processor requires resolvers only on the trackers' outer gimbal axes. The constant processor only requires the mechanization of constants which are sign-controlled as a function of the outer gimbal angles.

The use of the three processors to derive attitude control signals for an example satellite such as the Orbiting Astronomical Observatory is investigated. The functional requirements of the "coarse pointing mode" are imposed. It is shown that both the ideal and partial processor provide the required transient and steady-state performance over a commanded gimbal range that is limited only by the physical nature of the star tracker. Also, it is shown that resolver errors of 5° in the mechanization of the partial processor have a negligible effect on the performance of the system. The constant processor is shown to provide a system with the required performance over a commanded gimbal angle range of $\pm 60^{\circ}$.

INTRODUCTION

An important class of satellites is one whose mission requires that the satellite orientation be fixed with respect to inertial space. Such a vehicle is usually termed "inertially oriented" or "inertially stabilized." Mission objectives for this type of satellite frequently require extremely accurate attitude control, thus a precision sensor is needed for determining attitude.

One feasible sensor is the star tracker. The use of star trackers for attitude stabilization is the subject of this paper.

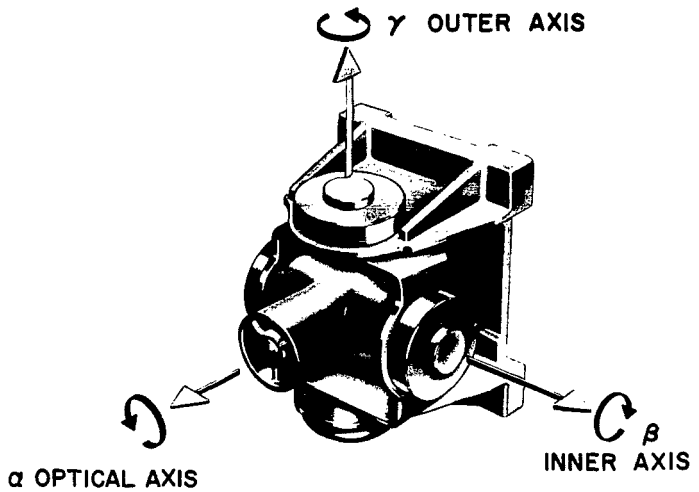

Figure 1.- Star tracker with two degrees of freedom.

The star tracker is an optical or light sensing device mounted in a gimbaled unit that has two degrees of freedom (fig. 1). The star tracker is locked onto a target star by sensing the misalinement between its optical axis and the line-of-sight (LOS) to the star and by using this error signal to drive the gimbals, the star tracker controls its optical axis to be coincident with the LOS to the star.

The attitude of a satellite can be related, in general, to a reference frame formed by the directions to two stars. If two star trackers are pointed at known guide stars and if the orientations of the star trackers with respect to the vehicle are known, the attitude of the satellite can be determined. Conversely, if the vehicle is in a desired attitude, the relative orientations of the two star trackers with respect to the vehicle can be calculated in terms of their gimbal angles. If the calculated gimbal angles are the commanded angles, the deviation of the gimbals from their commanded angles then provides a measure of the satellite's deviation from its prescribed attitude. At least three of the four gimbal angle errors from the two star trackers are required to determine the vehicle attitude error. Since the gimbal angle errors are generated about axes which are, in general, neither alined to the control axes of the vehicle nor mutually orthogonal, they must be processed to be useful as control signals.

Computation of the satellite attitude errors from the gimbal angle errors is quite complex if the exact equations are used. An approximate relationship is desired that simplifies the computation. If, however, the satellite attitude and guide stars for the trackers are to be arbitrary, then the gimbal error processor must provide useful control signals over a wide range of star tracker gimbal angles. Yet, if the processor is to be used on board a satellite, it should be as simple as possible.

The use of star trackers to derive control signals for satellite stabilization or attitude control has been studied in references 1 to 3. Meyer developed a scheme that can be used either to stabilize the attitude of the satellite or to control it through large-angle reorientation maneuvers. Since the method is general, computation of the control signals is complex and requires a computer on board the satellite. The processor developed in references 2 and 3 is much simpler to mechanize and does not require a computer.

It is, however, applicable only for attitude stabilization. The scheme is derived on the basis of a first-order approximation of the satellite from its nominal or prescribed attitude. Each star tracker provides an independent estimate of the satellite's error in attitude. Since a minimum of two trackers is required, the individual estimates are averaged to provide an approximation to the attitude error. Although its mechanization is simple, the scheme does not allow attitude stabilization of the satellite over the complete range of gimbal angles, since instabilities can occur when the commanded gimbal angles become large.

This paper considers three related processors of gimbal angle errors. They are like the processor in references 2 and 3, in that they come from a perturbation analysis where only first-order terms are considered significant. They differ, however, in that they process gimbal angle errors from pairs of star trackers rather than from each tracker independently. Of the three methods of processing the gimbal angle errors, the first, called the ideal processor, is a direct mechanization of the first-order approximation to the exact equations. The other two schemes, called the partial processor and the constant processor, are variations of the ideal processor that simplify the mechanization and eliminate the need for a computer. The ideal processor does require more computation than the simplified forms. The characteristics of the system using each of the processors are developed so that the choice of a particular processor for a specific application can be made by the system designer.

The first section of the report discusses the problem of determining a satellite's attitude by means of star trackers. The pertinent attitude perturbation equations are derived and various conditions that simplify their form are examined. The three processors are then defined and their peculiarities discussed. The next section concerns the design and performance analysis of a system using each of the three processors. Here the functional requirements and basic stabilization system parameters of the Orbiting Astronomical Observatory are used for illustration. Finally, a section is devoted to the results of a computer simulation of the example stabilization system using each of the three processors.

SYMBOLS

B1,B2	parameter plane variables for ideal and partial processor
B_D,B_T	parameter plane variables for partial processor - imperfect mechanization
cγ	cosine γ
C_D,C_T	parameter plane variables for constant processor - trackers 1 and 3
CE	characteristic equation

d_{13}	constant gain for partial processor - trackers 1 and 3
D_{ij}	determinant of N matrix for trackers i and j
E_D, E_T	parameter plane variables for constant processor - trackers 1 and 2
F_{12}	determinant of N matrix for trackers 1 and 2 when a gimbal error combination of $\Delta\beta_1$, $\Delta\gamma_1$, and $\Delta\gamma_2$ is used
g	linear transfer function for forward loop
g_i	nonlinear transfer function for forward loop
G	matrix transfer function for forward loop
H	product of constant processor and geometry matrix
H_D	determinant of H matrix
I	identity matrix
I_1	principal axis or control axis inertia
J	inertia of the motor inertia wheel
K	linear forward loop gain
K_c	compensator gain
K_m	motor gain
K_{si}	feedback gain when the partial processor is used
M	ideal processor
M_c	constant processor
M_p	partial processor
M_{PE}	partial processor - imperfect mechanization
N	geometry matrix
N_i	describing function for ith channel
q_{ij}	constants for constant processor - trackers 1,2
r_{ij}	constants for constant processor - trackers 1,3
R	transformation relating star tracker gimbal rates and vehicle rates

s	complex variable of the Laplace transformation
$s\gamma$	sine γ
$t\beta$	tangent β
t_i	external torque about the ith axis (time domain)
T_i	external torque about the ith axis ("s" domain)
u_{11}, u_{13}	constants in the partial processor for trackers 1 and 2
v_{11}, v_{13}	constants in the partial processor for trackers 1 and 3
$\alpha_i, \beta_i, \gamma_i$	rotations about the 1, 2, and 3 axes of the ith star tracker
$\dot{\alpha}_i, \dot{\beta}_i, \dot{\gamma}_i$	angular velocity about the 1, 2, and 3 axes of the ith star tracker
δ	measure of the partial processor mechanization error
$\Delta\alpha_i, \Delta\beta_i, \Delta\gamma_i$	first-order approximation to rotation about the 1, 2, and 3 axes of the ith star tracker
$\Delta\gamma_i$	error in the γ_i gimbal angle
$\Delta\gamma_R$	region of restricted operation
$(\Delta\varphi, \Delta\theta, \Delta\psi)$ or (φ, θ, ψ)	first-order approximation to rotations about control axes
$(\varphi_o, \theta_o, \psi_o)$	initial values of φ, θ, and ψ
$\epsilon_\varphi, \epsilon_\theta, \epsilon_\psi$	control signals obtained from the processors
ζ	relative damping ratio
$\dot{\varphi}, \dot{\theta}, \dot{\psi}$	angular rates about the control axes
τ_1, τ_2	compensator time constants
τ_m	motor time constant
$\omega_{1v}, \omega_{2v}, \omega_{3v}$	inertial angular rate of the vehicle
$\omega_{w1}, \omega_{w2}, \omega_{w3}$	angular rate of the motor inertia wheel
ω_{wio}	initial angular rate of the ith motor inertia wheel
ω_n	natural frequency

ATTITUDE DETERMINATION VIA STAR TRACKERS

The role of the star trackers in the control system is depicted in sketch (a). The star trackers, represented by one block in the sketch, are considered to be locked onto selected target stars. When the vehicle is in its desired attitude, the trackers point away from the satellite in the directions corresponding to the gimbal angles which are selected on the ground and stored in the vehicle as commands. But since various disturbances move the vehicle while the trackers still point at their targets, the gimbal angles differ from their commanded values. The sketch illustrates that these angle errors are detected and processed to form an estimate of the vehicle's deviation from its desired attitude. Finally, the sketch shows that this estimate is used by the controller to activate a motor or jet, which, in turn, drives the vehicle back to its desired attitude.

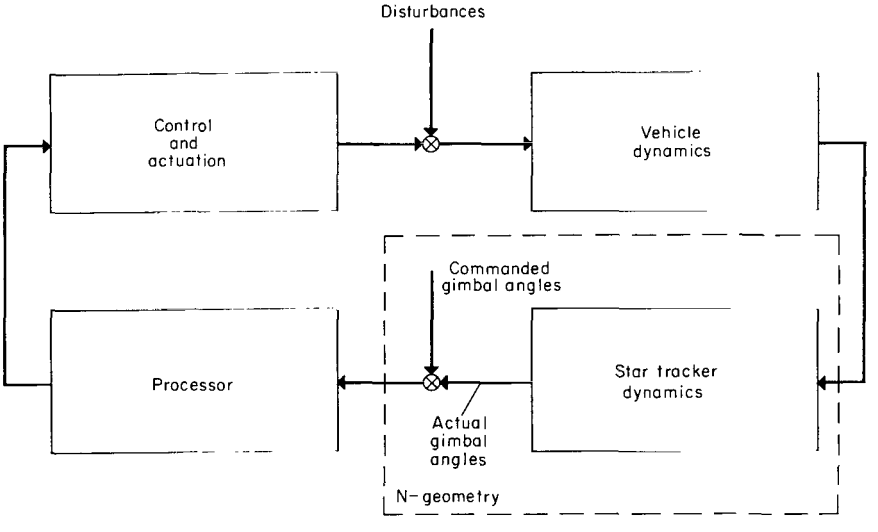

Sketch (a)

The forms of the geometry matrix, N, and the processor matrix depend on the way the star trackers are mounted on the vehicle. Figure 2 illustrates the mounting arrangements considered in this report, defining them relative to the vehicle's control axes (1^V - roll, 2^V - pitch, 3^V - yaw). The trackers are shown with their gimbal axes in the null position and their optical, inner, and outer axes labeled 1, 2, and 3, respectively. The superscript indicates the tracker number; thus, 1^2 is the optical axis of tracker number 2. Trackers 1, 2, and 3 are mounted to the vehicle similarly: their outer gimbal axes (3^i) are alined to the roll axis (1^V) of the vehicle. Tracker 4 is mounted differently: its outer gimbal axis, 3^4, is parallel to the pitch axis (2^V) of the vehicle.

The orientation of a star tracker with respect to the vehicle is specified by two gimbal angles. The angles for tracker number 1 are defined in the drawing on the right in figure 2. The inner and outer gimbal angles are

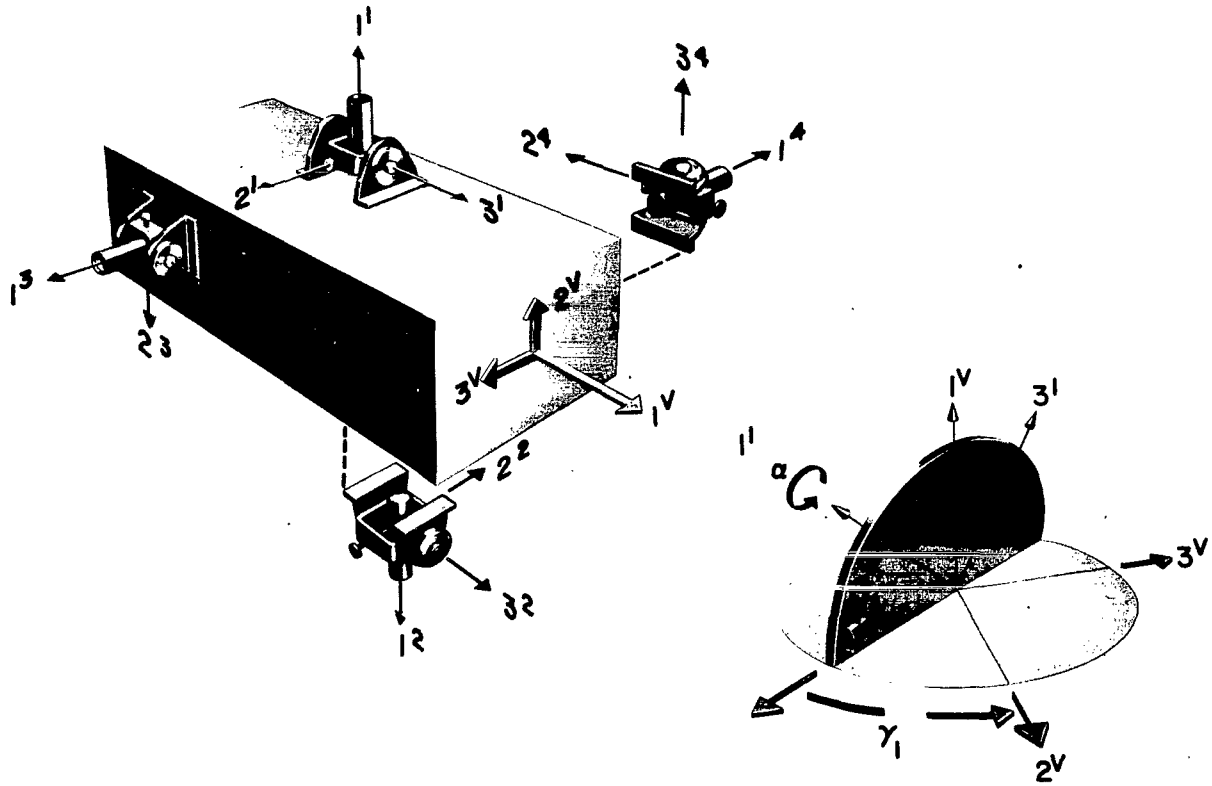

Figure 2.- Illustration of gimbal angles and arrangements of star trackers on the spacecraft.

designated, β_1 and γ_1, respectively. To define a coordinate system for the star tracker, a third angle (α_1) is introduced which refers to angular rotation about the optical axis. The angle α_1 cannot be measured by the star tracker. Angles for the other trackers are similarly defined.

The motion of the satellite can be expressed both in the coordinate system defined in the vehicle and in the coordinate system defined in the tracker. A simple way of describing the motion is to express the angular velocity of the vehicle (ω_{1v}, ω_{2v}, ω_{3v}) in terms of the gimbal angle rates of the star tracker ($\dot{\alpha}_1$, $\dot{\beta}_1$, $\dot{\gamma}_1$). In order to equate the gimbal angle rates to the vehicle angular rates, it must be assumed that the sensor tracks its star perfectly. The sensor's error signal, which this assumption ignores, can easily be added later if necessary. The transformation between tracker gimbal rates and vehicle angular rates is derived in appendix A. The rate transformation, R, for each of the trackers indicated in figure 2 is given in table I. Since the control system is to be used for stabilization and the motion about any nominal attitude can be considered small, a perturbation analysis is appropriate. Therefore, the vehicle angular rates (ω_{1v}, ω_{2v}, ω_{3v}) are approximated by

the Euler angle rates $(\dot{\varphi}, \dot{\theta}, \dot{\psi})$. Since the motion is assumed to be small, trigonometric elements in the transformation R can be considered constants that are evaluated at the nominal or commanded angles. The transformation R then provides a first-order approximation to the relationship between the deviation of the gimbal angles from their commanded values and the deviation of the satellite from its prescribed attitude. For example, the first-order approximation for tracker number 1 is

$$\begin{bmatrix} \Delta\alpha_1 \\ \Delta\beta_1 \\ \Delta\gamma_1 \end{bmatrix} = \begin{bmatrix} 0 & c\gamma_1/c\beta_1 & -s\gamma_1/c\beta_1 \\ 0 & s\gamma_1 & c\gamma_1 \\ 1 & -c\gamma_1 t\beta_1 & s\gamma_1 t\beta_1 \end{bmatrix} \begin{bmatrix} \Delta\varphi \\ \Delta\theta \\ \Delta\psi \end{bmatrix} \tag{1}$$

The attitude error of the vehicle could be determined from equation (1) if each of the error signals $\Delta\alpha_1$, $\Delta\beta_1$, and $\Delta\gamma_1$ were measured by the star tracker. Since the star tracker cannot sense angular motion about its optical axis, $\Delta\alpha_1$ is not measurable. A gimbal angle error signal from a second star tracker must then be substituted for $\Delta\alpha_1$ to determine the vehicle attitude. The third measurable signal could be either an outer gimbal error signal $(\Delta\gamma)$ or an inner gimbal error signal $(\Delta\beta)$ from any of the remaining trackers. For example, if the inner gimbal error from star tracker 3 $(\Delta\beta_3)$ is substituted for $\Delta\alpha_1$, the following transformation is obtained:

$$\begin{bmatrix} \Delta\beta_1 \\ \Delta\gamma_1 \\ \Delta\beta_3 \end{bmatrix} = \begin{bmatrix} 0 & s\gamma_1 & c\gamma_1 \\ 1 & -c\gamma_1 t\beta_1 & s\gamma_1 t\beta_1 \\ 0 & -c\gamma_3 & s\gamma_3 \end{bmatrix} \begin{bmatrix} \Delta\varphi \\ \Delta\theta \\ \Delta\psi \end{bmatrix} \tag{2}$$

The attitude of the vehicle can now be estimated from the gimbal angle measurements (if they form an independent set) by inverting equation (2).

Equation (2) gives a form that matrix N can take. Several forms arising from different combinations of gimbal error signals from two trackers are given in table II; many other combinations are also possible. For example, one error signal from each of three star trackers could be used to estimate the error in vehicle attitude. However, the use of gimbal errors from three trackers has a distinct disadvantage when reliability is considered. Consequently, gimbal error signals from only two trackers are considered. The gimbal error combinations listed in table II are representative of all the possible cases.

If the gimbal freedom of the star trackers is restricted to small angles and if the trackers are properly mounted to the vehicle, the gimbal error signals directly provide an accurate estimate of the attitude error. However, it is usually desirable to be able to command large gimbal angles to track the available guide stars. Therefore, the gimbal axes are, in general, not alined to the control axes nor do they form an orthogonal set. A transformation is then required to convert the gimbal error signals into an estimate of the vehicle attitude error. Three classes of such transformations, or processors, are defined. They are referred to as (1) the ideal processor, (2) the partial processor, and (3) the constant processor.

Ideal Processor

The ideal processor is defined as the first-order approximation relating the vehicle control signals to the gimbal angle errors. For tracker pair 1,3 when the gimbal errors $\Delta\beta_1$, $\Delta\gamma_1$, and $\Delta\beta_3$ are used, the processor is the inverse of equation (2) and is given by the following equation:

$$\begin{bmatrix} \epsilon_\varphi \\ \epsilon_\theta \\ \epsilon_\psi \end{bmatrix} = \frac{1}{c(\gamma_1-\gamma_3)} \begin{bmatrix} s(\gamma_3-\gamma_1)t\beta_1 & c(\gamma_1-\gamma_3) & -t\beta_1 \\ s\gamma_3 & 0 & -c\gamma_1 \\ c\gamma_3 & 0 & s\gamma_1 \end{bmatrix} \begin{bmatrix} \Delta\beta_1 \\ \Delta\gamma_1 \\ \Delta\beta_3 \end{bmatrix} \qquad (3)$$

The ideal processor for the other combinations of gimbal angle errors is given as the M matrix in table II. Each is the inverse of the corresponding N matrix.

The processor (M) could be mechanized on the satellite in at least two ways. The first method would be to mechanize each of the matrix elements with a potentiometer whose values would be programmed for each desired attitude. The potentiometers could be programmed either manually from a ground station or automatically on board the satellite. In either case, additional telemetry channels are required. Manual programming from a ground station has the advantage that an on board memory unit is not required but the disadvantage that changes in attitude can be made only when the satellite is over a ground station. Automatic programming of the potentiometers has the advantage that changes in the desired attitude can be made at any position in the orbit but the disadvantage that a memory unit is required. The size of the memory unit depends on the number of changes in desired attitude between ground stations and the number of tracker pairs that must be programmed. The second method

would be to mechanize the trigonometric elements actively. Although such mechanization is more complex than that with potentiometers, a storage unit and additional telemetry channels are not required. Also, attitude can be changed at any position in orbit. The theoretical investigation that follows is applicable to either mechanization.

The complexity of the ideal processor varies with the particular gimbal error combination selected. For example, the ideal processor for tracker pair 1,2 - if $\Delta\beta_1$, $\Delta\gamma_1$, and $\Delta\beta_2$ are used - is

$$\begin{bmatrix} \epsilon_\varphi \\ \epsilon_\theta \\ \epsilon_\psi \end{bmatrix} = \frac{1}{s(\gamma_1-\gamma_2)} \begin{bmatrix} c(\gamma_1-\gamma_2)t\beta_1 & s(\gamma_1-\gamma_2) & t\beta_1 \\ c\gamma_2 & 0 & c\gamma_1 \\ -s\gamma_2 & 0 & -s\gamma_1 \end{bmatrix} \begin{bmatrix} \Delta\beta_1 \\ \Delta\gamma_1 \\ \Delta\beta_2 \end{bmatrix} \tag{4}$$

and has the same form as equation (3). The processors in equations (3) and (4) are clearly simpler than the other ideal processors listed in table II. The simpler processors have not only two zero elements but also simpler trigonometric functions for the nonzero elements.

The complexity of the ideal processor depends on both the relative alinement of the paired star trackers and on the combination of gimbal errors chosen to estimate the attitude error. Although many combinations were studied, only representative cases are discussed. The variation in complexity due to the relative alinement of the paired trackers is revealed by comparing the processors for tracker pairs 1,3 and 1,4. Since both use a gimbal error combination of two inner and one outer, the simpler processor of tracker pair 1,3 clearly indicates the preferred alinement occurs when the outer gimbal axes are parallel. The variation in complexity due to the combination of gimbal errors then is exhibited by comparing the two processors for tracker pair 1,2. The simpler processor is obtained when a gimbal error combination of two inner ($\Delta\beta_1$, $\Delta\beta_2$) and one outer ($\Delta\gamma_1$) is used. In summary, therefore, the simplest ideal processor is obtained when the paired star trackers are mounted to the vehicle so that their outer gimbal axes are parallel and when a combination of two inner and one outer gimbal error signals is chosen. Mechanizing this processor insures that, to a first order, the control channels are decoupled.

Partial Processor

Mechanization of even the simplest form of the ideal processor for use on board a spacecraft is relatively complex due to the appearance of such functions as the sine and cosine of the difference of angles and the tangent. It is usually desirable to obtain a simpler form that still provides the necessary performance. Simpler forms are obtained by considering approximations to the ideal processor. If, to reduce complexity, only simple sine and cosine terms in the ideal processor are mechanized by using resolvers, while the more complex elements are made constant, the transformation in equation (3) can be written

$$M_p = \begin{bmatrix} v_{11} & 1 & v_{13} \\ d_{13}s\gamma_3 & 0 & -d_{13}c\gamma_1 \\ d_{13}c\gamma_3 & 0 & d_{13}s\gamma_1 \end{bmatrix} \tag{5}$$

where v_{11} is the constant for $-[s(\gamma_1-\gamma_3)/c(\gamma_1-\gamma_3)]t\beta_1$, v_{13} is the constant for $[-t\beta_1/c(\gamma_1-\gamma_3)]$, and d_{13} is the constant for $[1/c(\gamma_1-\gamma_3)]$. The constants (v_{11}, v_{13}, d_{13}) are independent of the gimbal angles. Equation (5) is designated the partial processor. The product of the partial processor and the geometry matrix is

$$M_pN = \begin{bmatrix} 1 & (v_{11}s\gamma_1-c\gamma_1t\beta_1-v_{13}c\gamma_3) & (v_{11}c\gamma_1+s\gamma_1t\beta_1+v_{13}s\gamma_3) \\ 0 & d_{13}c(\gamma_1-\gamma_3) & 0 \\ 0 & 0 & d_{13}c(\gamma_1-\gamma_3) \end{bmatrix} \tag{6}$$

It follows from equation (6) that this processor insures the independence of only two control signals (ϵ_θ and ϵ_ψ) rather than all three as obtained with the ideal processor. However, the loss of independence of ϵ_φ is a small price to pay for the simpler mechanization. Equation (6) also shows that the gains of ϵ_θ and ϵ_ψ through the partial processor are functions of the commanded outer gimbal angles, whereas their gains through the ideal processor are constant. Consequently, the dynamic response of the system using the partial processor varies as a function of the commanded outer gimbal angles.

The partial processor is the processor that provides two independent control signals when only the sine and cosine terms of the ideal processor are mechanized. It is derived from only the simplest ideal processor (table II). To use this processor, the inner gimbal error signal from one tracker is passed through a resolver on the outer gimbal of the second tracker of the pair; thus, $\Delta\beta_1$ is passed through the outer gimbal resolver of γ_3, and $\Delta\beta_3$ is passed through the outer gimbal resolver of γ_1.

Constant Processor

Although the partial processor allows simple mechanization, another approximation to the ideal processor allows even simpler mechanization. This form, designated as the constant processor, is obtained by letting each of the nonzero elements of the ideal processor be constant. The elements of the matrix are not parameters to be evaluated at each commanded set of gimbal angles. They are to remain constant at least in magnitude over the whole range of allowed values of the angles. However, the matrix elements have different signs in different regions of the range of angles. These sign changes will be discussed later. The constant processor for tracker pair 1,3 is

$$M_C = \begin{bmatrix} r_{11} & 1 & r_{13} \\ r_{21} & 0 & r_{23} \\ r_{31} & 0 & r_{33} \end{bmatrix} \tag{7}$$

where r_{11} is the constant for $-[s(\gamma_1-\gamma_3)/c(\gamma_1-\gamma_3)]t\beta_1$, r_{21} is the constant for $s\gamma_3/c(\gamma_1-\gamma_3)$, etc. Only seven of the nine matrix elements must be mechanized. The product matrix M_CN is

$$M_CN = \begin{bmatrix} 1 & (r_{11}s\gamma_1-c\gamma_1t\beta_1-r_{13}c\gamma_3) & (r_{11}c\gamma_1+s\gamma_1t\beta_1+r_{13}s\gamma_3) \\ 0 & (r_{21}s\gamma_1-r_{23}c\gamma_3) & (r_{21}c\gamma_1+r_{23}s\gamma_3) \\ 0 & (r_{31}s\gamma_1-r_{33}c\gamma_3) & (r_{31}c\gamma_1+r_{33}s\gamma_3) \end{bmatrix} \tag{8}$$

and shows that the pitch and yaw error signals are independent of the motion about the roll axis.

The constant processors derived from the simplest ideal processor (table II) not only simplifies the mechanization but also simplifies the analysis. The mechanization is simplified because only seven of the nine elements must be considered. The constant processors which might be derived from ideal processors other than the simplest require that all nine elements be mechanized. The analysis is simplified because the control signals are partially decoupled (see eq. (8)).

Indeterminant Condition

Since the gimbal axes vary as a function of the relative orientation of the star tracker and vehicle, the error signals do not, in general, form an orthogonal set of measurements and can, in fact, form a dependent set of measurements. When this occurs, the attitude of the vehicle is unobservable. This situation is termed the indeterminant condition.

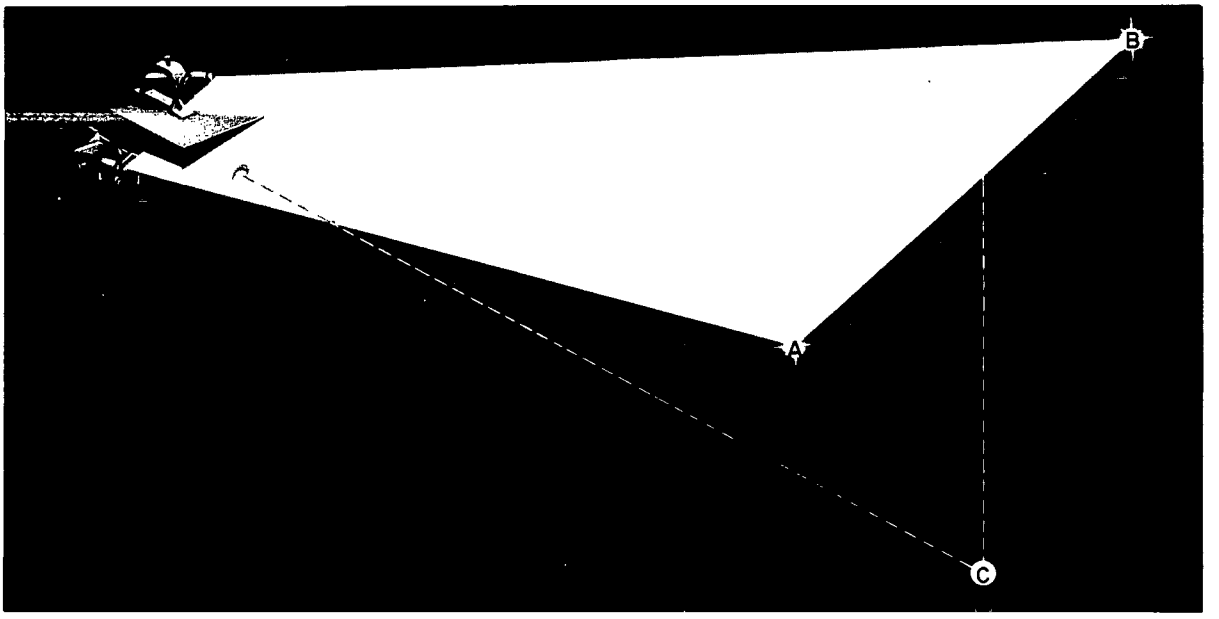

Figure 3.- Illustration showing when indeterminant condition would occur.

The indeterminant condition exists when the determinant of the N matrix vanishes. The indeterminancy is therefore independent of the processor. From the determinants given in table II (D_{12}, D_{13}, D_{14}, F_{12}), it can be seen that the condition is simplest to ascertain when the star trackers are used in a manner that provides the simplest ideal processor. For example, the indeterminant condition occurs for tracker pair 1,3 when $D_{13} = c(\gamma_1-\gamma_3) = 0$, for tracker pair 1,2 when $D_{12} = s(\gamma_1-\gamma_2) = 0$, and for tracker pair 1,4 when $D_{14} = s\gamma_1 s\gamma_4 - c\gamma_4 t\beta_1 = 0$. The geometrical interpretation of the indeterminant condition for the preferred design (D_{12} and D_{13}) is that the optical axes of the paired star trackers and the outer gimbal axes are coplanar. The situation would occur if the direction associated with point C in figure 3 were contained in the plane defined by the vehicle and the targets stars A and B. This interpretation provides a simple criterion for the selection of stars by ground operations to avoid the condition.

The vehicle cannot be operated within the neighborhood of the indeterminant condition because the error signals become less and less sensitive to some motions. For example, the indeterminant condition for tracker pair 1,3 occurs when $c(\gamma_1-\gamma_3) = 0$ or, equivalently, when $|\gamma_1-\gamma_3| = 90^\circ$. Therefore, the region in which vehicle operation is prohibited is defined as

$$90^\circ - \Delta\gamma_R \leq |\gamma_1-\gamma_3| \leq 90^\circ + \Delta\gamma_R \qquad (9)$$

where $\Delta\gamma_R$ defines the magnitude of the restricted region. A graphical interpretation of the restricted region is indicated by the shaded area in sketch (b).

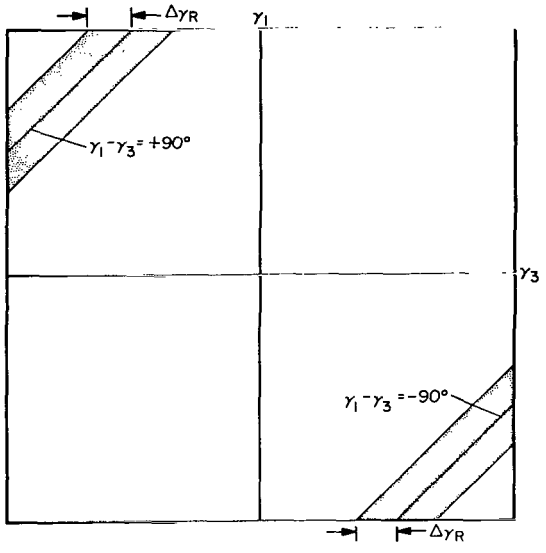

Sketch (b)

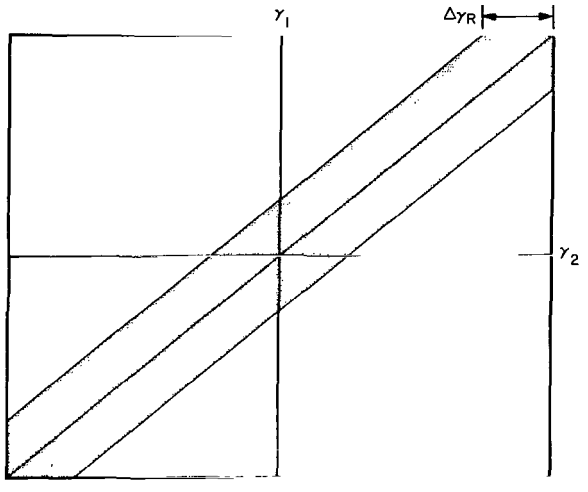

Sketch (c)

Similarly, the indeterminant condition for tracker pair 1,2 occurs when $s(\gamma_1-\gamma_2) = 0$ or $|\gamma_1-\gamma_2| = 0^o$. The restricted region is

$$|\gamma_1-\gamma_2| \leq \Delta\gamma_R \tag{10}$$

and is indicated by the shaded area in sketch (c).

ANALYSIS AND DESIGN

The use of the three processors in deriving control signals for attitude stabilization of an example satellite is investigated in this section. An example of a satellite that might use the processors developed in the previous section is the Orbiting Astronomical Observatory (OAO) whose mission objectives require that the experiments on the satellite be directed at arbitrary points in the celestial sphere. When the vehicle is pointed at an arbitrary target, the attitude is defined by gimbaled star trackers and is controlled by three mutually orthogonal motor inertia-wheel combinations. Both the stability and performance of the example system using each of the processors to derive control signals will be investigated. Although the example satellite uses momentum transfer for control, the use of the processors is not restricted to such a system.

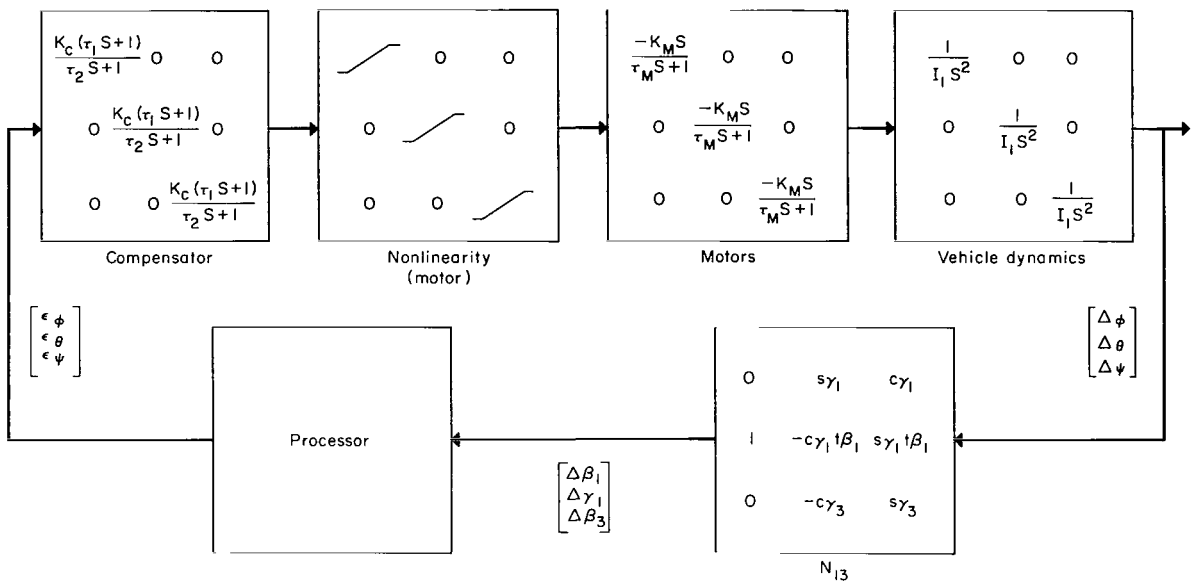

Figure 4.- Attitude control system using star trackers 1 and 3.

Figure 4 is a block diagram of the control system. The gimbal error signals from tracker pair 1,3 are shown being processed to provide an estimate of the attitude errors. The processor indicated on the diagram could be any one of the three discussed in the previous section, ideal, partial, or constant. The equations provided in the diagram assume the following conditions: (1) The mass distribution of the vehicle is such that the moments of inertia about any three orthogonal axes are equal; (2) the linearized equations validly describe the motor inertia-wheel combination; (3) the motor torque is limited; and (4) gyroscopic coupling due to inertial wheel rotation is negligible. A lead compensator is introduced because without it the system would be highly oscillatory.

The motor nonlinearity shown in figure 4 is represented by a describing function (ref. 4). This representation is valid since the motor-vehicle combination behaves as a low-pass filter. The describing function is a pure gain which decreases monotonically from its maximum value of unity - obtained with the input in the linear region - to zero as the input increases.

Ideal Processor

Stability.- Mechanization of the ideal processor insures that, to a first order, the error signals, ϵ_φ, ϵ_θ, and ϵ_ψ, are independent; that is, each error signal is only a function of the attitude error about its corresponding axis. For example, the product of the ideal processor M and the geometry N is the unity matrix. The control channels are therefore uncoupled and system

stability is determined by investigating each control loop independently. That this is true can be seen by deriving the characteristic equation (CE).

$$CE = DET(I + GMN) = 0 \tag{11}$$

where

$$MN = I \tag{12}$$

$$G = \begin{bmatrix} g_1 & 0 & 0 \\ 0 & g_2 & 0 \\ 0 & 0 & g_3 \end{bmatrix} \tag{13}$$

$$g_i = \frac{N_i K(\tau_1 s + 1)}{s(\tau_2 s + 1)(\tau_m s + 1)} \qquad i = 1, 2, 3 \tag{14}$$

N_i = describing function for the ith channel

$$K = \frac{K_c K_m}{I_1} \tag{15}$$

Equation (11) can be written as follows:

$$CE = (1 + g_1)(1 + g_2)(1 + g_3) = 0 \tag{16}$$

Since the motion is damped if all roots of the characteristic equation have negative real parts, it is necessary to show that the roots of each factor in equation (16) have negative real parts. A general expression for the factors is

$$(1 + g_i) = 0 \qquad i = 1, 2, 3 \tag{17}$$

Substituting equation (14) into equation (17) gives:

$$s^3 + \left(\frac{1}{\tau_2} + \frac{1}{\tau_m}\right) s^2 + \left(\frac{1}{\tau_2 \tau_m} + \frac{10 N_i K}{\tau_m}\right) s + \frac{N_i K}{\tau_2 \tau_m} = 0 \tag{18}$$

where

$$\tau_1 = 10\tau_2$$

The parameter plane method (ref. 5) is convenient for determining stability. This method allows the system's stability to be expressed as a function of two variable parameters. If the two variable parameters are defined by the following equations,

$$\left.\begin{aligned} B1 &= 1/\tau_2 \\ B2 &= N_i K \end{aligned}\right\} \tag{19}$$

the characteristic equation can be written as follows:

$$s^3 + \left(B1 + \frac{1}{\tau_m}\right) s^2 + \left(\frac{B1}{\tau_m} + \frac{10B2}{\tau_m}\right) s + \frac{B1B2}{\tau_m} = 0 \tag{20}$$

By substituting $-\omega_n\zeta + j\omega_n\sqrt{1 - \zeta^2}$ for s and equating the real and imaginary parts of the resulting expression for equation (20) to zero, the variable parameters can be expressed as functions of damping (ζ) and natural frequency (ω_n) for a particular value of τ_m. Thus, contours of constant ζ can be mapped as functions of B1 and B2 with the $\zeta = 0$ contour defining the stability boundary.

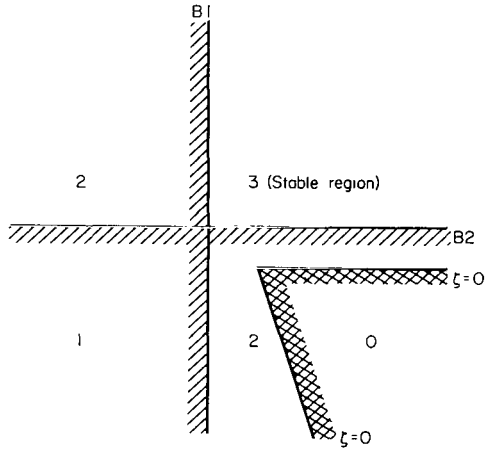

Sketch (d)

The stability regions on the parameter plane are obtained by determining both the real root boundaries ($\sigma = 0$ and $\sigma = \infty$) and the complex root boundaries ($\zeta = 0$). Real root boundaries (ref. 5) occur at $B1 = 0$ and $B2 = 0$ and are plotted along with the complex root boundaries in sketch (d). If the boundaries are properly shaded,[1] the number of stable roots (roots with negative real parts) can be determined for any combination of B1 and B2. The numbers in the sketch indicate the number of stable roots in each region. Since the characteristic equation is third order, the sketch shows that the system is stable, provided both B1 and B2 are positive. An expanded plot of this first quadrant is given in figure 5.

The stability of the system using the ideal processor is determined by examining the range of the variable parameters (B1, B2). It is observed from equation (19) that B1 and B2 are always positive because τ_2, N_i, and K are always positive. Since the describing function N_i varies from zero to one, the operating point of the system varies along a constant B1 line from $B2 \approx 0$ (large errors) to $B2 = K$ (linear region) but is always in the first quadrant. The system is, therefore, stable.

[1]The shading of stability boundaries is opposite to that suggested in reference 5.

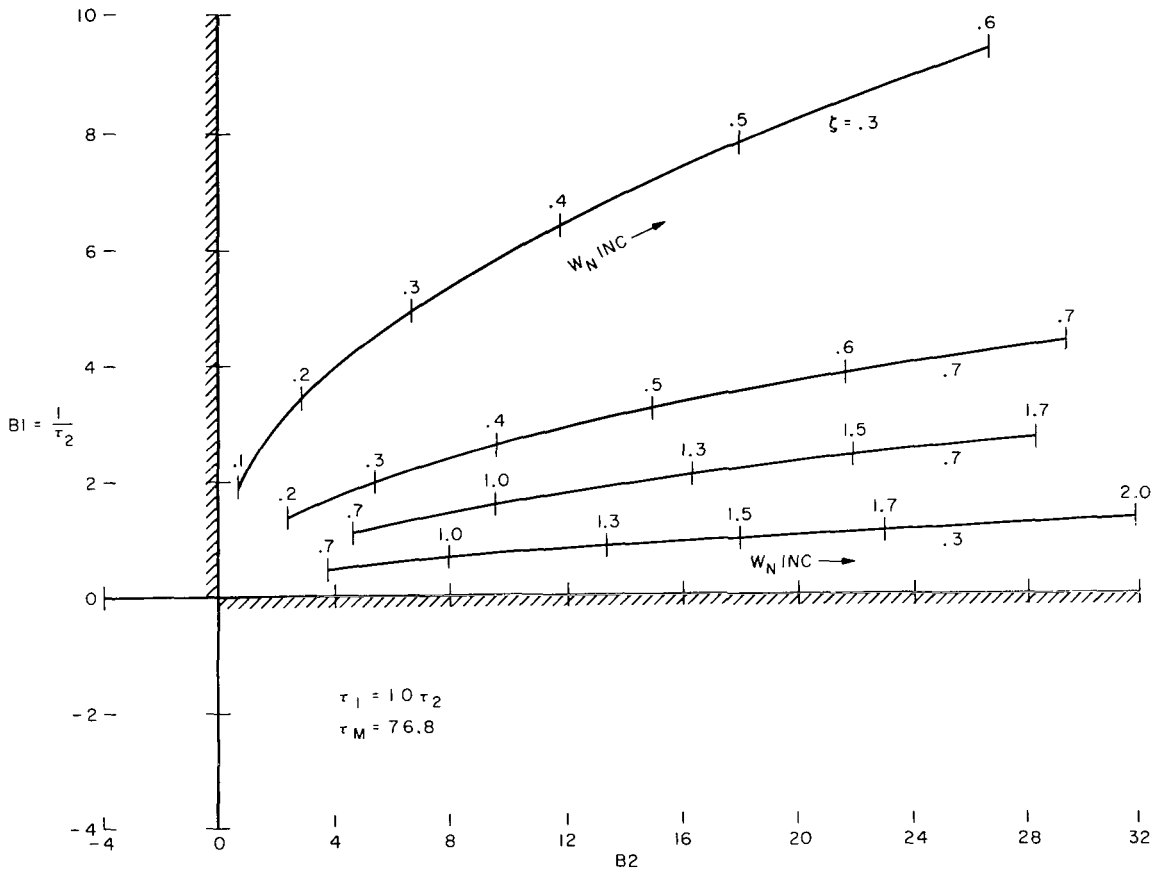

Figure 5.- Parameter plane for ideal and partial processor.

Practical considerations require that certain gimbal angles should not be commanded. The analysis just concluded implies that the system is stable for any range of commanded gimbal angles. Although this is true, mechanization of the ideal processor requires the term $1/c(\gamma_1-\gamma_3)$ to be mechanized. Since $[1/c(\gamma_1-\gamma_3)] \rightarrow \infty$ as $|\gamma_1-\gamma_3| \rightarrow 90^{\circ}$, an upper limit must be imposed on the gain term. This limit has already been established in the discussion on the indeterminant condition and was defined as the region of restricted operation in the γ_1, γ_3 plane.

The simultaneous use of multiple tracker pairs in the control loop may be desirable for reliability purposes. The advantage of using more than one pair of trackers is that the malfunction of one tracker will not result in the loss of vehicle control. If several pairs are used simultaneously, the

estimated attitude error signals from each pair of trackers may be averaged. For example, if the loop gains for tracker pair 1,2 and 1,3 are, respectively, $B2_{12}$ and $B2_{13}$, the loop gain for the multiple pair system is

$$B2_{av} = \frac{B2_{12} + B2_{13}}{2} \tag{21}$$

Since the B2 for any individual tracker pair is positive, the average is positive. The system using multiple pairs of trackers is therefore stable.

Performance.- The system using the ideal processor has been shown to be stable. It is now necessary to choose the parameters B1 and B2 that will provide the desired transient and steady-state performance.

The OAO telescope is alined with the roll axis of the vehicle. Since the telescope must point accurately in some specific direction, two stringent steady-state conditions are imposed on the pitch and yaw channels. The first condition, called Pointing Accuracy, requires that the roll axis of the vehicle be pointed to within ±1 min of arc. The second condition, called Drift Rate Accuracy, requires that the desired attitude be held to within 15 sec of arc for 50 minutes of time.

The steady-state errors are obtained by applying the final value theorem to the pitch and yaw transfer functions when the torque input is a step function. The pointing error and drift rate error are

$$\sqrt{\theta_{ss}^2 + \psi_{ss}^2} = \sqrt{\left(\frac{\dot{\theta}_o + \frac{J}{I_1}\omega_{w2o}}{K}\right)^2 + \left(\frac{\dot{\psi}_o + \frac{J}{I_1}\omega_{w3o}}{K}\right)^2} \leq PE \tag{22}$$

$$\sqrt{\dot{\theta}_{ss}^2 + \dot{\psi}_{ss}^2} = \sqrt{\left(\frac{t_2}{I_1 K}\right)^2 + \left(\frac{t_3}{I_1 K}\right)^2} \leq DR \tag{23}$$

where ω_{w2o} and ω_{w3o} are initial wheel speeds for pitch and yaw motors; "ss" refers to steady state; t_2 and t_3 are external torques about the pitch and yaw axes; and PE and DR are the maximum acceptable pointing error and the maximum acceptable drift rate error, respectively. In addition, it is assumed that the steady-state motion is in the linear region so that $N_1 = 1$. Equations (22) and (23) rewritten as

$$B2\big|_{PE} = K\big|_{PE} \geq \frac{1}{PE}\left[\left(\dot{\theta}_o + \frac{J}{I_1}\omega_{w2o}\right)^2 + \left(\dot{\psi}_o + \frac{J}{I_1}\omega_{w3o}\right)^2\right]^{1/2} \tag{24}$$

$$B2\big|_{DR} = K\big|_{DR} \geq \frac{1}{DR}\left[\left(\frac{t_2}{I_1}\right)^2 + \left(\frac{t_3}{I_1}\right)^2\right]^{1/2} \tag{25}$$

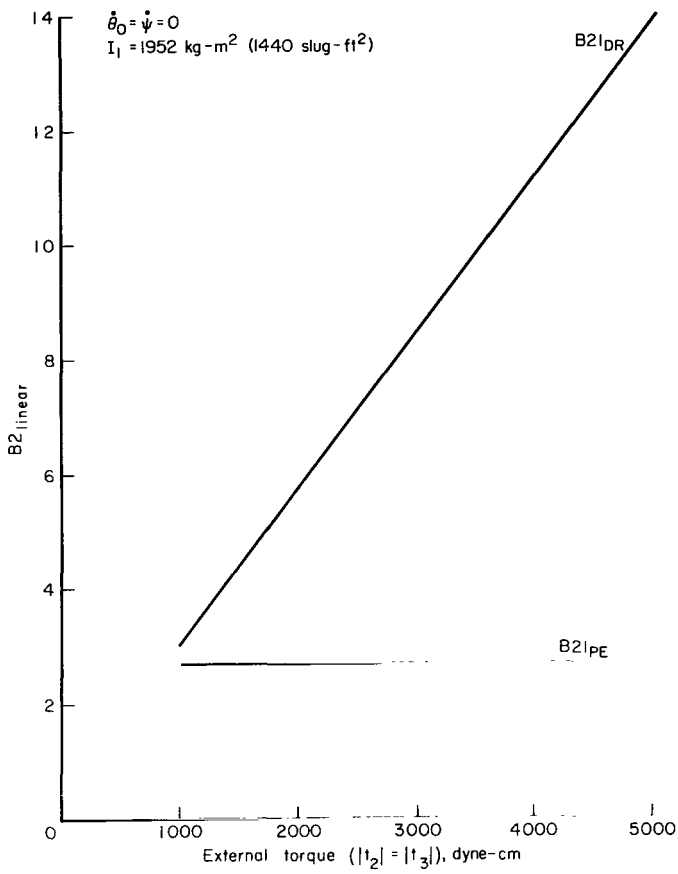

Figure 6.- Steady-state gain requirements - ideal and partial processor.

specify the minimum gain K (or minimum B2) necessary to satisfy each of the steady-state conditions. The minimum gain (K) calculated from equations (24) and (25) is plotted in figure 6 for the conditions listed in table III. For example, if $|\omega_{w2O}|$ = 40 percent of the maximum wheel speed and if $|t_2|$ = 1000 dyne-cm, the minimum gains (K) necessary to satisfy the pointing accuracy and the drift rate accuracy are, respectively, K = 2.7 and K = 3.0. Therefore, the minimum gain that satisfies the drift rate specification also satisfies the pointing accuracy specification. This minimum gain is equivalent to the minimum value of B2 in the linear region (N_i = 1). A value of B1 must then be chosen in the acceptable range of B2 so that the vehicle exhibits the desired transient performance in the pitch and yaw channels; that is, a B1 and B2 (N_i = 1) are selected from the parameter plane in figure 5 so that the desired damping ratio and natural frequency are obtained.

Since the observatory is alined to the roll axis of the vehicle, performance in roll is not so critical as in pitch and yaw. However, the procedure for designing the roll control channel is identical to the procedure just described for the pitch and yaw channels.

Partial Processor With Perfect Mechanization

Stability.- The characteristic equation (CE) for the system using the partial processor is derived as follows:

$$CE = DET(I + GM_PN) = 0 \tag{26}$$

The expanded form of the characteristic equation, with tracker pair 1,3, is

$$(1 + g_1)[1 + g_2d_{13}c(\gamma_1-\gamma_3)][1 + g_3d_{13}c(\gamma_1-\gamma_3)] = 0 \tag{27}$$

where the g_i are given by equation (14). Since the stability of the system is determined by investigating the roots of the individual products, the following generalized form is defined.

$$(1 + K_{si}g_i) = 0 \tag{28}$$

where

$$K_{si} = \begin{cases} 1 & i = 1 \\ d_{13}c(\gamma_1-\gamma_3) & i = 2, 3 \end{cases} \tag{29}$$

Equation (14) can be used to write equation (28) as

$$s^3 + \left(\frac{1}{\tau_2} + \frac{1}{\tau_m}\right) s^2 + \left(\frac{1}{\tau_2\tau_m} + \frac{10N_iK_{si}K}{\tau_m}\right) s + \frac{KN_iK_{si}}{\tau_2\tau_m} = 0 \tag{30}$$

where $\tau_1 = 10\tau_2$.

The parameter plane is used to determine stability. If the variable parameters are defined as follows,

$$\left.\begin{aligned} B1 &= \frac{1}{\tau_2} \\ B2 &= N_iK_{si}K \end{aligned}\right\} \tag{31}$$

equation (30) becomes identical to equation (20). Therefore, the regions of stability defined on the parameter plane for the partial processor are identical to the regions defined for the ideal processor (sketch (d) and fig. 5). The difference between the behavior of the system using the processors lies in the variability of the parameter K_{si} (cf. eqs. (31) and (19)).

The system using the partial processor is then stable if the parameters B1 and B2 are always positive. Clearly, the parameter B1 is positive. Since N_i and K are positive, the condition $B2 > 0$ is satisfied if $K_{si} > 0$. The condition is satisfied for the roll channel ($K_{si} = 1$). For the pitch and yaw channels, the condition $K_{si} > 0$ requires that the sign of d_{13} be controlled as follows:

$$d_{13} \gtrless 0 \quad \text{if} \quad |\gamma_1-\gamma_3| \lesssim 90^\circ \tag{32}$$

The parameter B2 is then positive for all three control channels and the system is stable.

The following observations are made from the preceding analysis. First, the two constants v_{11} and v_{13} in the partial processor for tracker pair 1,3 do not affect the stability of the system. They do, however, influence the

amount of pitch and yaw motion that is coupled into the roll channel (see eq. (6)). To give v_{11} and v_{13} values other than zero in the hope of minimizing the coupling leads either to complex logic or to computation equivalent to mechanizing the ideal processor. Henceforth, they will be set equal to zero. Second, the technique of combining outputs from multiple pairs of trackers when using the ideal processor may be applied successfully when using the partial processor.

Performance.- The parameters must now be chosen so that the system will exhibit the desired transient and steady-state performance. Using the definitions of steady-state error from the previous section, inequalities analogous to equations (24) and (25) are

$$B2\big|_{PE} = KK_{s2}\big|_{PE} \geq \frac{1}{PE}\left[\left(\dot{\theta}_o + \frac{J}{I_1}\omega_{w2o}\right)^2 + \left(\dot{\psi}_o + \frac{J}{I_1}\omega_{w3o}\right)^2\right]^{1/2} \tag{33}$$

$$B2\big|_{DR} = KK_{s2}\big|_{DR} \geq \frac{1}{DR}\left[\left(\frac{t_2}{I_1}\right)^2 + \left(\frac{t_3}{I_1}\right)\right]^{1/2} \tag{34}$$

where

$$K_{s2} = K_{s3} \quad \text{(see eq. (29))}$$

Equations (33) and (34) provide the minimum loop gain KK_{s2} necessary to satisfy, respectively, the pointing accuracy requirement and the drift rate requirement. The system will satisfy both steady-state requirements if the magnitude of the gain is chosen at least as large as the larger of the gains specified by equations (33) and (34); that is,

$$B2 \geq \max\left\{KK_{s2}\big|_{PE}\ ,\ KK_{s2}\big|_{DR}\right\} \tag{35}$$

where

$$N_i = 1 \quad \text{(linear region)}$$

The transient performance of the system varies with the relative orientation of the star trackers and vehicle because of the variation in loop gain (B2). The desired transient performance must be achieved over the complete range of parameters. Assuming that the minimum B2 is chosen in the range specified by equation (35), equation (31) becomes

$$Kd_{13} = \frac{B2_{min}}{[c(\gamma_1-\gamma_3)]_{min}} \tag{36}$$

where the minimum value of $c(\gamma_1-\gamma_3)$ is dictated by the magnitude of the restricted region. The maximum value of B2 is

$$B2_{max} = Kd_{13} = \frac{B2_{min}}{[c(\gamma_1-\gamma_3)]_{min}} \tag{37}$$

A value of B1 is chosen from the parameter plane (fig. 5) so that acceptable transient performance in pitch and yaw is achieved over the complete range of B2. The pitch and yaw channels then exhibit both the desired transient and steady-state performance. The desired performance in roll is not so stringent as pitch and yaw and is easily achieved.

The system using the partial processor for other tracker pairs exhibits performance identical to that just found for tracker pair 1,3. Also, the design procedure is identical. The only difference between tracker pairs occurs in the definition of K_{si}. If the paired trackers are mounted on perpendicular faces of the vehicle, the gain $K_{si} = d_{jk}c(\gamma_j-\gamma_k)$. If the paired trackers are mounted on parallel faces of the vehicle, the gain $K_{si} = d_{jk}s(\gamma_j-\gamma_k)$.

Partial Processor With Imperfect Mechanization

General.- The partial processor, if perfectly mechanized, provides a system that stabilizes the satellite over a range of commanded gimbal angles limited only by the possible angular rotation of the gimbals. Since errors in mechanization exist, it is desired to determine their effect on the stability and performance of the system. Mechanization of the partial processor involves passing the gimbal error signals through resolvers and through fixed gain elements (pots or amplifiers). The fixed gain elements are assumed to be perfectly mechanized and the errors in mechanization exist only in the resolvers. Imperfect mechanization results from either the misalinement of the resolvers or an inaccurate readout of the gimbal position and would appear as a resolver angle of $\gamma + \Delta\gamma$ where $\Delta\gamma$ represents the error. The errors are assumed to be less than 5° so that only the first-order terms are significant.

The partial processor for tracker pair 1,3 with errors in mechanization is

$$M_{PE} = \begin{bmatrix} 0 & 1 & 0 \\ d_{13}s(\gamma_3+\Delta\gamma_3) & 0 & -d_{13}c(\gamma_1+\Delta\gamma_1) \\ d_{13}c(\gamma_3+\Delta\gamma_3) & 0 & d_{13}s(\gamma_1+\Delta\gamma_1) \end{bmatrix} \tag{38}$$

The product of the processor matrix (M_{PE}) and the geometry matrix (N) would show that the errors in mechanization have the effect of coupling the pitch and yaw channels. The effect of the errors on the stability and performance of the system is now investigated.

Stability.- The characteristic equation (CE) for the system using the partial processor for tracker pair 1,3 with errors in mechanization is

$$CE = DET(I + GM_{PE}N) = 0 \tag{39}$$

The expanded form of equation (39) is derived in appendix B (B9) and is

$$CE = (1 + gN_1)(1 + B_T g + B_D g^2) = 0 \tag{40}$$

where

$$g = \frac{K(\tau_1 s + 1)}{s(\tau_2 s + 1)(\tau_m s + 1)} \tag{41}$$

$$B_T = (N_2 + N_3)d_{13}c(\gamma_1-\gamma_3) + d_{13}(c\gamma_3 s\gamma_1 N_2 - s\gamma_3 c\gamma_1 N_3)\delta \tag{42}$$

$$B_D = N_2 N_3 d_{13}c(\gamma_1-\gamma_3)[d_{13}c(\gamma_1-\gamma_3) + d_{13}s(\gamma_1-\gamma_3)\delta] \tag{43}$$

$$\delta = (\Delta\gamma_3-\Delta\gamma_1) \tag{44}$$

Parameters B_T and B_D are also derived in appendix B ((B14) and (B16)) and are obtained by considering only the first-order error terms as significant. The parameter δ, defined by equation (44), is a measure of the error in mechanization. The coupling introduced by the mechanization errors precludes factoring the second-order polynomial in g (see eq. (40)) into two first-order polynomials. (Compare equation (27) for perfect mechanization.)

The stability of the system is determined by investigating the factors in equation (40). Since the roots of the factor $(1 + gN_1) = (1 + g_1)$ have already been shown to be stable, it is only necessary to investigate the polynomial

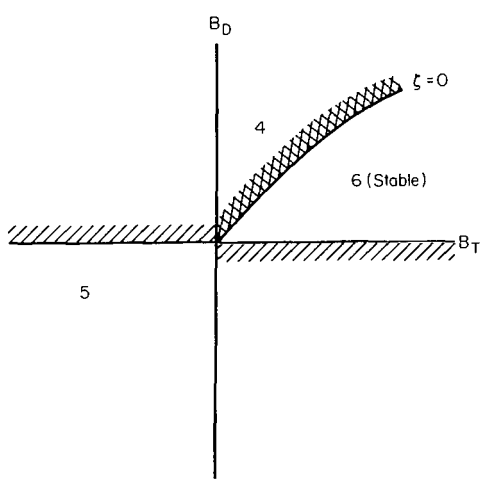

Sketch (e)

$$1 + B_T g + B_D g^2 = 0 \tag{45}$$

System stability can be expressed as a function of the two parameters B_T and B_D by using the parameter plane method. The real and complex boundaries as well as the number of stable roots for each region are shown in sketch (e). Since the polynomial of equation (45) is sixth order when expanded, any combination of B_T and B_D that remains in the first quadrant but below the $\zeta = 0$ curve provides a stable system. An expanded plot of the first quadrant is given in figure 7.

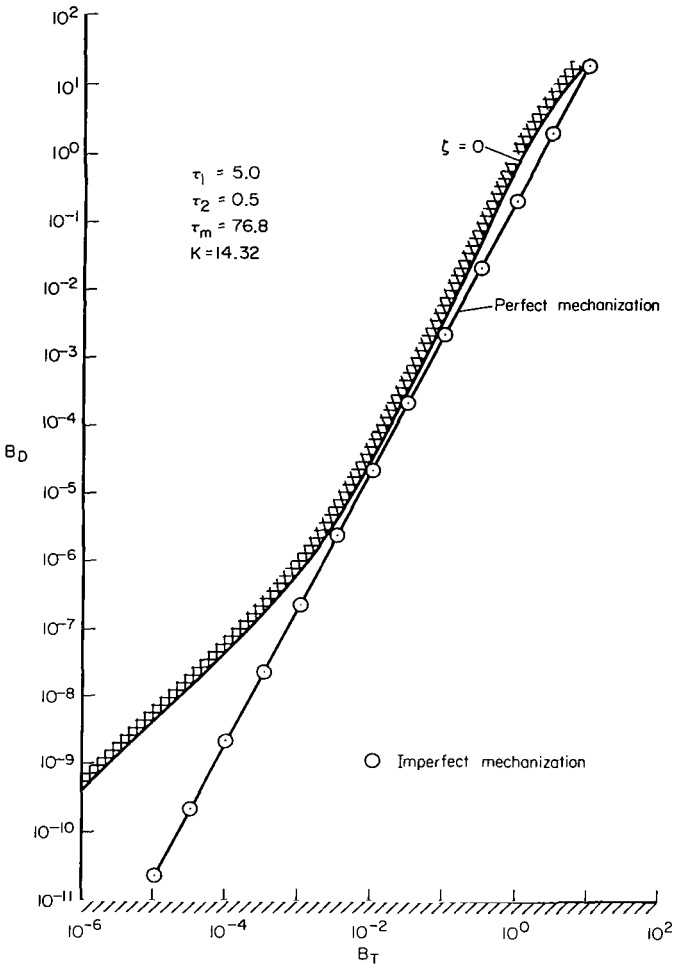

Figure 7.- Parameter plane - partial processor - trackers 1,3.

The stability of the system is determined by calculating the range of the parameters B_T and B_D. If the actual parameters are contained within the stable region indicated in sketch (e), the system is stable. Both the minimum and the maximum B_D must be calculated for a given B_T. If $B_{D_{max}}$ is less than the $\zeta = 0$ boundary and if $B_{D_{min}} > 0$, the system is stable.

For comparison purposes, the stability of the system with perfect mechanization is determined before imperfections are introduced. The system has already been shown to be stable. The difference between the previous analysis and the present analysis is in the definition of the equations used to express stability. For perfect mechanization, equations (42) and (43) become the following:

$$B_T = (N_2 + N_3)d_{13}c(\gamma_1-\gamma_3) \quad (46)$$

$$B_D = N_2N_3[d_{13}c(\gamma_1-\gamma_3)]^2 \quad (47)$$

Since the maximum B_D for a given B_T occurs when $N_2 = N_3$, equations (46) and (47) can be combined to give

$$B_{D_{max}} = \left(\frac{B_T}{2}\right)^2 \quad (48)$$

The maximum B_D is plotted as the solid line on the parameter plane in figure 7. Since the minimum B_D is positive, the system is, as previously indicated, stable.

The stability of the system with errors in mechanization is determined next. Since a closed-form solution for the maximization of B_D does not exist, the equations were programmed on a computer. The maximum B_D was calculated for a fixed B_T over the range of parameters considered; that is, $-60^\circ \le \gamma_1,\gamma_3 \le +60^\circ$, $1.11\times10^{-5} \le N_2,N_3 \le 1$ (equivalent to initial attitude errors as large as 5°), and mechanization errors of $0 \le |\Delta\gamma_1|, |\Delta\gamma_3| \le 5^\circ$. For gimbal angle errors of $|\Delta\gamma_1| = |\Delta\gamma_3| = 5^\circ$, figure 7 indicates an

insignificant difference in maximum B_D due to imperfections. The minimum B_D is made positive by selecting the magnitude of the restricted region ($\Delta\gamma_R$). Since $B_{D_{min}} > 0$, the following inequality is derived from (43)

$$|\delta|_{max} < |\cot(\gamma_1-\gamma_3)|_{min} \tag{49}$$

where the minimum value of the cotangent is determined by the magnitude of the restricted region ($\Delta\gamma_R$). If $|\Delta\gamma_1| = -|\Delta\gamma_3|$, (49) can be written

$$2|\Delta\gamma_1|_{max} < |\cot(\gamma_1-\gamma_3)|_{min} \tag{50}$$

If $|\Delta\gamma_R| = 10^\circ$, the right side of (50) is evaluated at $|\gamma_1-\gamma_3| = 90^\circ \pm 10^\circ$. The maximum gimbal angle error is therefore

$$|\Delta\gamma_1|_{max} < 5.05^\circ$$

Therefore, $B_{D_{min}}$ is always positive and the system is stable for any mechanization error less than 5°.

Performance.- The performance of the system could be severely affected if large errors in mechanization existed and were not considered. For example, assume that the system with perfect mechanization is designed so that the steady-state requirements are just met at the minimum loop gain, which occurs on the boundary of the restricted region. If errors in mechanization actually do exist, the system could be operating in the restricted zone and would not exhibit the required steady-state performance. Therefore, the region in which gimbal angles cannot be commanded must be expanded by an amount equivalent to the maximum mechanization errors; thus, the region of restricted operation is

$$90^\circ - (|\Delta\gamma_R| + |\delta|_{max}) \leq |\gamma_1-\gamma_3| \leq 90^\circ + (|\Delta\gamma_R| + |\delta|_{max}) \tag{51}$$

Constant Processor With Tracker Pairs Mounted on Perpendicular Faces

Constraints on the constants.- The stability of the system deriving its error signals from the constant processor for tracker pair 1,3 is determined in this section. The characteristic equation (CE) is

$$CE = DET(I + GM_cN) = 0 \tag{52}$$

where

$$M_c = \begin{bmatrix} r_{11} & 1 & r_{13} \\ r_{21} & 0 & r_{23} \\ r_{31} & 0 & r_{33} \end{bmatrix}$$

or, equivalently,

$$CE = (1 + gN_1)(1 + C_T g + C_D g^2) = 0 \tag{53}$$

where

$$C_T = N_2(r_{21}s\gamma_1 - r_{23}c\gamma_3) + N_3(r_{31}c\gamma_1 + r_{33}s\gamma_3) \tag{54}$$

$$C_D = N_2N_3(r_{21}r_{33} - r_{31}r_{23})c(\gamma_1-\gamma_3) \tag{55}$$

and the r_{ij} are constants to be determined.

Except for the definitions of the constants, equations (53) and (40) are the same. Therefore, the following two conclusions can be extracted from the analysis for the partial processor (imperfect mechanization). First, the elements r_{11} and r_{13} can be equated to zero because they influence only the coupling between the control channels and not the stability of the system. Second, the stable ranges of variation of the parameters C_T and C_D are the same as those of B_T and B_D because the systems have the same parameter plane diagram. The diagram for the constant processor given in figure 8 shows not only the stability boundary illustrated in figure 7 and sketch (e), but also the curve for $\zeta = 0.2$.

The parameters C_T and C_D must, at least, be positive for the system to be stable. This requirement can be met only if the signs of the constants are controlled as a function of the outer gimbal angles γ_1 and γ_3. Since N_2 and N_3 are positive, the following inequalities, which are the 22 and 33 elements of the product matrix M_cN (see eq. (8)),

$$(r_{21}s\gamma_1 - r_{23}c\gamma_3) > 0 \tag{56}$$

$$(r_{31}c\gamma_1 + r_{33}s\gamma_3) > 0 \tag{57}$$

are sufficient to insure that C_T remain positive. Since mechanization simplicity is desired, arbitrarily let $r_{21} = 0$. Inequality (56) is satisfied if r_{23} is negative since the gimbal range is $-60^\circ \leq \gamma_1,\gamma_3 \leq +60^\circ$. It follows from equation (55) that the parameter C_D will always be positive if the sign of the constant r_{31} is controlled as follows.

$$r_{31} \gtrless 0 \quad \text{if} \quad |\gamma_1-\gamma_3| \lesssim 90^\circ \tag{58}$$

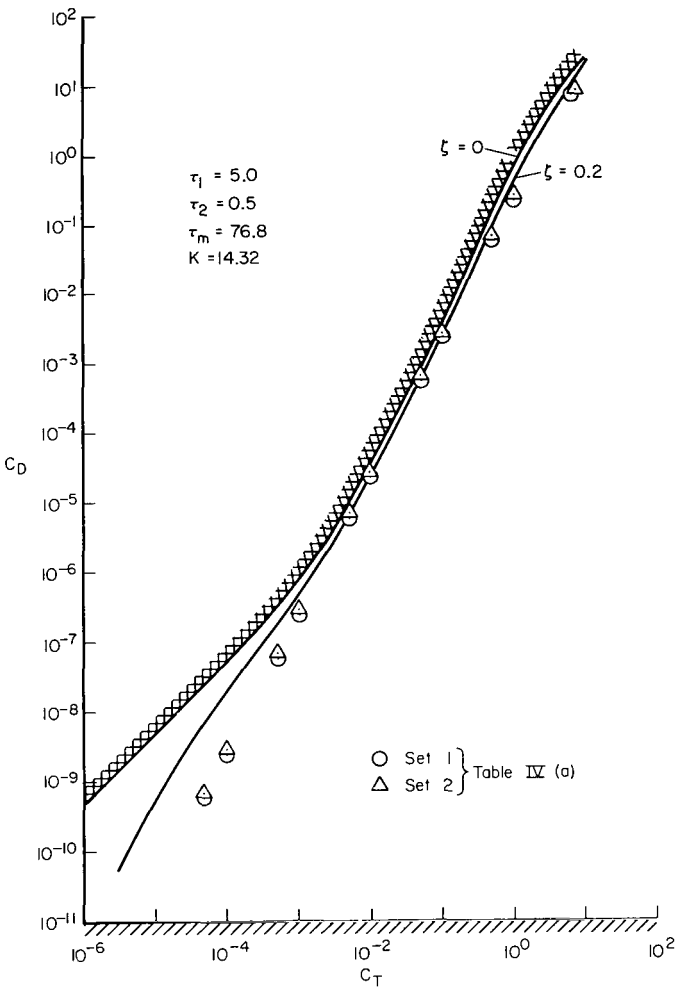

Figure 8.- Parameter plane - constant processor - trackers 1,3.

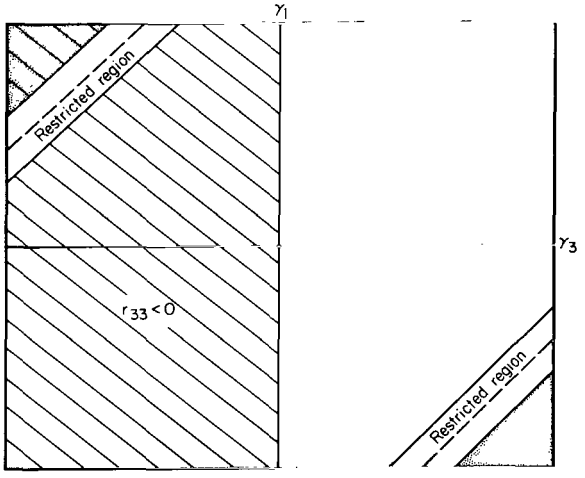

Sketch (f)

Because r_{31} can be negative, the following two conditions must be imposed on r_{33} to satisfy the inequality (57). First, the sign of the constant r_{33} must be controlled as follows:

$$r_{33} \gtrless 0 \quad \text{if} \quad \gamma_3 \gtrless 0 \qquad (59)$$

or $r_{33}s\gamma_3 > 0$. Second, the magnitude of r_{33} must be chosen so that the inequality of (60) is satisfied.

$$|r_{33}| > \left(\left| \frac{c\gamma_1}{s\gamma_3} \right|_{\substack{\max \\ r_{31} < 0}} \right) |r_{31}| \qquad (60)$$

The region in which (60) must be evaluated is shaded in sketch (f); that is, the region in which $r_{31} < 0$. Also indicated on the sketch is the sign of the constants as a function of the gimbal angles (γ_1, γ_3) and the region of restricted operation. Evaluating the inequality of (60) for the worse condition ($\gamma_1 = +40^\circ$ and $\gamma_3 = -60^\circ$) results in

$$|r_{33}| > 0.884|r_{31}| \qquad (61)$$

Therefore, the parameters C_D and C_T are positive if $r_{21} = 0$, $r_{23} < 0$, and inequalities (58), (59), and (61) are satisfied.

The parameters C_D and C_T are positive but the system is not necessarily stable. The constants (r_{23}, r_{31}, r_{33}) must be chosen so that the range of C_D and C_T is contained within the stable operating region indicated on the parameter plane

(fig. 8). Searching for a set of constants over an unrestricted range that will provide a stable system is impractical. The range of constants over which the search must be made is reduced considerably by investigating only those sets that provide the desired steady-state performance.

Steady-state performance.- The equations describing the steady-state pointing error and the steady-state drift rate error for the system using the constant processor are derived in appendix C and are given by

$$\sqrt{\theta_{ss}^2 + \psi_{ss}^2} = \frac{1}{H_D K} \sqrt{(h_{33}h_{20} - h_{23}h_{30})^2 + (-h_{32}h_{20} + h_{22}h_{30})^2} \leq PE \quad (62)$$

$$\sqrt{\dot{\theta}_{ss}^2 + \dot{\psi}_{ss}^2} = \frac{1}{H_D K} \sqrt{\left(h_{33}\frac{t_2}{I_1} - h_{23}\frac{t_3}{I_1}\right)^2 + \left(-h_{32}\frac{t_2}{I_1} + h_{22}\frac{t_3}{I_1}\right)^2} \leq DR \quad (63)$$

where

$H = h_{ij} = M_c N$ for tracker pair 1,3

$H_D = (r_{21}r_{33} - r_{23}r_{31})c(\gamma_1 - \gamma_3)$

t_i = external torque about the ith axis

$$\begin{bmatrix} h_{1o} \\ h_{2o} \\ h_{3o} \end{bmatrix} = \begin{bmatrix} \dot{\varphi}_o - \frac{J}{I_1}\omega_{w1o} \\ \dot{\theta}_o - \frac{J}{I_1}\omega_{w2o} \\ \dot{\psi}_o - \frac{J}{I_1}\omega_{w3o} \end{bmatrix}$$

h_{io} is proportional to the initial momentum about the ith axis. If H_D and the elements of the H matrix are substituted for trackers 1,3 (eq. (8)) and $r_{21} = 0$, equations (62) and (63) can be written as quadratic equations in r_{23} as follows:

$$\{h_{3o}^2 - [(PE)Kr_{31}c(\gamma_1 - \gamma_3)]^2\}r_{23}^2 - \{2[r_{33} - r_{31}s(\gamma_1 - \gamma_3)]h_{2o}h_{3o}\}r_{23} + [r_{31}^2 + r_{33}^2 - 2r_{31}r_{33}s(\gamma_1 - \gamma_3)]h_{2o}^2 \leq 0 \quad (64)$$

$$\{t_3^2 - [(DR)I_1Kr_{31}c(\gamma_1 - \gamma_3)]^2\}r_{23}^2 - \{2[r_{33} - r_{31}s(\gamma_1 - \gamma_3)]t_2t_3\}r_{23} + [r_{31}^2 + r_{33}^2 - 2r_{31}r_{33}s(\gamma_1 - \gamma_3)]t_2^2 \leq 0 \quad (65)$$

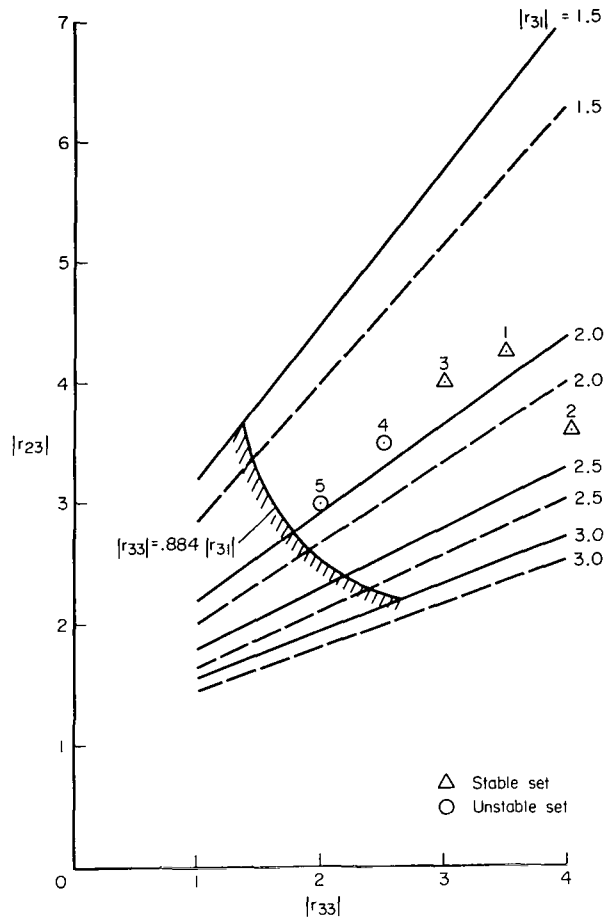

Figure 9.- Steady-state gain requirements - constant processor - trackers 1,3.

Sets of constants (r_{23}, r_{31}, r_{33}) can then be calculated so that the system will satisfy each of the individual steady-state requirements for the most severe conditions. These conditions are listed in table III. The acceptable range of r_{23} for a given r_{31} and r_{33} is plotted in figure 9. The solid lines of constant $|r_{31}|$ indicate the minimum $|r_{23}|$ for a given $|r_{33}|$ to satisfy the drift rate specification. The dashed lines provide the same information for the pointing accuracy specifications. For example, if $|r_{31}| = 2.0$ and $|r_{33}| = 3.0$, the drift rate accuracy requires that $|r_{23}| \geq 3.65$ and the pointing accuracy requires that $|r_{23}| \geq 3.32$. In general, the $|r_{23}|$ that satisfies the drift rate specification also satisfies the pointing accuracy specification.

Stability.- The stability of the system is now investigated by calculating the range of the variable parameters (C_T, C_D) for a specific set of constants chosen from the acceptable region. The acceptable region is defined as the region that satisfies not only the steady-state conditions but also the inequality of (61). The hatched boundary in figure 9 is plotted for the condition that $|r_{33}| = 0.884\ |r_{31}|$. Therefore, for a given r_{33}, acceptable sets of constants are chosen from the region to the right of the hatched boundary and above the constant r_{31} boundary. The sets of constants investigated are listed in table IV(a). Sets 1, 2, and 3 provide a stable system whereas sets 4 and 5 result in an unstable system. The "worst case" results of the stability calculations for sets 1 and 2 are plotted on the parameter plane in figure 8. The sets are also shown on figure 9 with an indication of system stability (the △ indicates a stable set and the "o" indicates an unstable set). The figure shows that sets of constants that assure stable operation begin to occur when the left side of (57) becomes significantly positive.

Constant Processor With Tracker Pair Mounted on Parallel Faces

Constraints on the constants.- The stability and performance of a system using trackers 1 and 2 is investigated next. The characteristic equation is identical to equation (52) except that M_c and N are defined for trackers 1,2 (table II). Therefore, the form of equation (53) for trackers 1,2 is

$$CE = (1 + gN_1)(1 + E_T g + E_D g^2) = 0 \tag{66}$$

where

$$E_T = N_2(q_{21}s\gamma_1 - q_{23}s\gamma_2) + N_3(q_{31}c\gamma_1 - q_{33}c\gamma_2) \tag{67}$$

$$E_D = N_2N_3(q_{23}q_{31} - q_{21}q_{33})s(\gamma_1-\gamma_2) \tag{68}$$

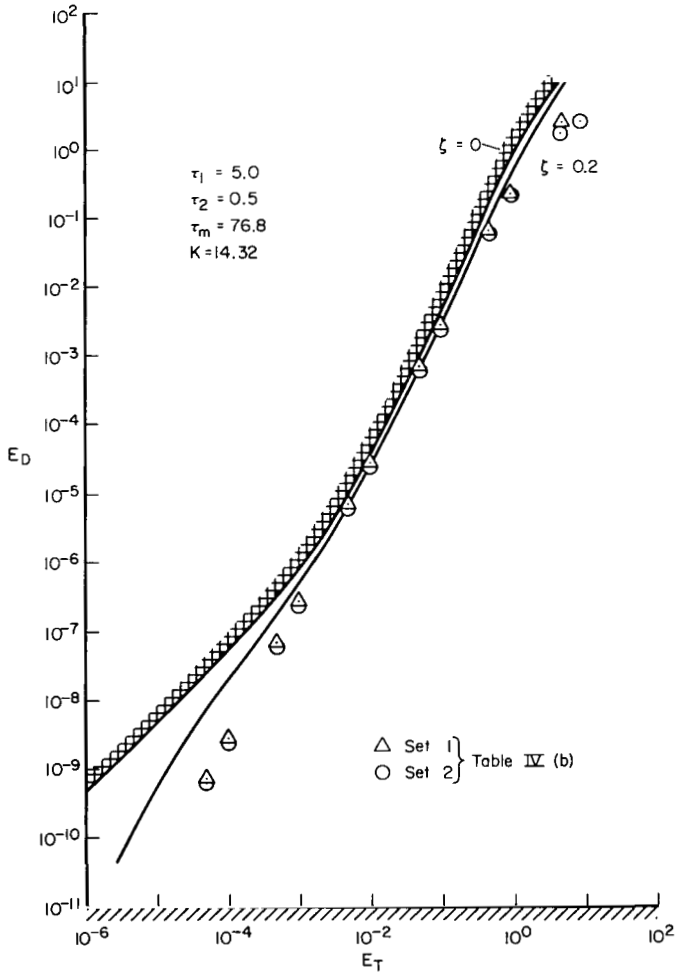

Figure 10.- Parameter plane - constant processor - trackers 1,2.

As in the previous case, the constants q_{11} and q_{13} are equated to zero. Also, the parameter plane diagram for the system, using the constant processor for trackers 1,2 (E_T, E_D), is identical to the diagram for the imperfect mechanization of the partial processor (sketch (e) or fig. 7) and is given by figure 10.

A necessary condition for stability is that E_T, $E_D > 0$. The parameter E_T is positive if the following inequalities are satisfied.

$$q_{21}s\gamma_1 - q_{23}s\gamma_2 > 0 \tag{69}$$

$$q_{31}c\gamma_1 - q_{33}c\gamma_2 > 0 \tag{70}$$

To simplify the mechanization, let $q_{21} = q_{23}$. The inequality of (69) is satisfied if the constants q_{21} and q_{23} are controlled as follows.

$$q_{23} = q_{21} \gtrless 0 \quad \text{if} \quad (\gamma_1-\gamma_2) \gtrless 0 \tag{71}$$

The parameter E_D is then positive if

$$(q_{31}-q_{33}) > 0 \tag{72}$$

It remains to insure that the inequality of (70) is satisfied. It follows that (70) and (72) are satisfied if q_{31} and q_{33} are chosen as indicated below.

$$q_{31} > q_{33} > 0 \quad \text{if} \quad |\gamma_1| < |\gamma_2| \tag{73}$$

$$q_{33} < q_{31} < 0 \quad \text{if} \quad |\gamma_1| > |\gamma_2| \tag{74}$$

Parameters E_D and E_T are then positive. The sign of the constants as well as the region of restricted operation is plotted as a function of the outer gimbal angles in sketch (g); also $q_{31}, q_{33} < 0$ is shaded area and $q_{21} > 0$ is cross hatched area.

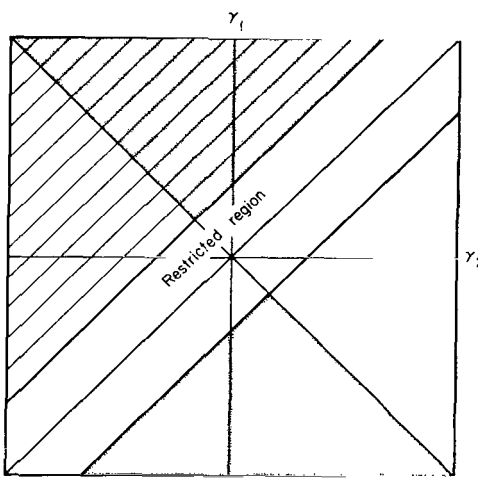

Sketch (g)

Steady-state performance.- The equations for steady-state pointing accuracy and steady-state drift rate accuracy are given, respectively, by equations (62) and (63) where H and H_D are now defined for trackers 1 and 2; that is

$$H = h_{ij} = M_c N \quad \text{for tracker pair 1,2}$$

$$H_D = q_{21}(q_{31}-q_{33})s(\gamma_1-\gamma_2)$$

Substituting the elements of the H matrix into equations (62) and (63) yields

$$\{[PEK(q_{31}-q_{33})s(\gamma_1-\gamma_2)]^2 - 2[1 - c(\gamma_1-\gamma_2)]h_{30}^2\}q_{21}^2$$

$$+ (\{2(q_{31}+q_{33})[1 - c(\gamma_1-\gamma_2)]\}h_{20}h_{30})q_{21} - [q_{31}^2 + q_{33}^2 - 2q_{31}q_{33}c(\gamma_1-\gamma_2)]h_{20}^2 \geq 0 \tag{75}$$

$$\left\{[DRK(q_{31}-q_{33})s(\gamma_1-\gamma_2)]^2 - 2[1 - c(\gamma_1-\gamma_2)]\left(\frac{t_3}{I_1}\right)^2\right\} q_{21}^2$$

$$+ \left(\{2(q_{31}+q_{33})[1 - c(\gamma_1-\gamma_2)]\}\frac{t_2}{I_1}\frac{t_3}{I_1}\right) q_{21}$$

$$- [q_{31}^2 + q_{33}^2 - 2q_{31}q_{33}c(\gamma_1-\gamma_2)]\left(\frac{t_2}{I_1}\right)^2 \geq 0 \tag{76}$$

(These equations are also given by equations (C23) and (C24) in appendix C.) The acceptable region of q_{21} for a given q_{31} and q_{33} can then be determined for the most severe condition from equations (75) and (76). If the equations are evaluated at the conditions listed in table III, the most severe condition is determined by scanning the range of gimbal angles and by controlling the sign of the input parameters (t_i and h_{io}). The constant (q_{21}) that satisfies the most severe condition is plotted in figure 11, where the solid

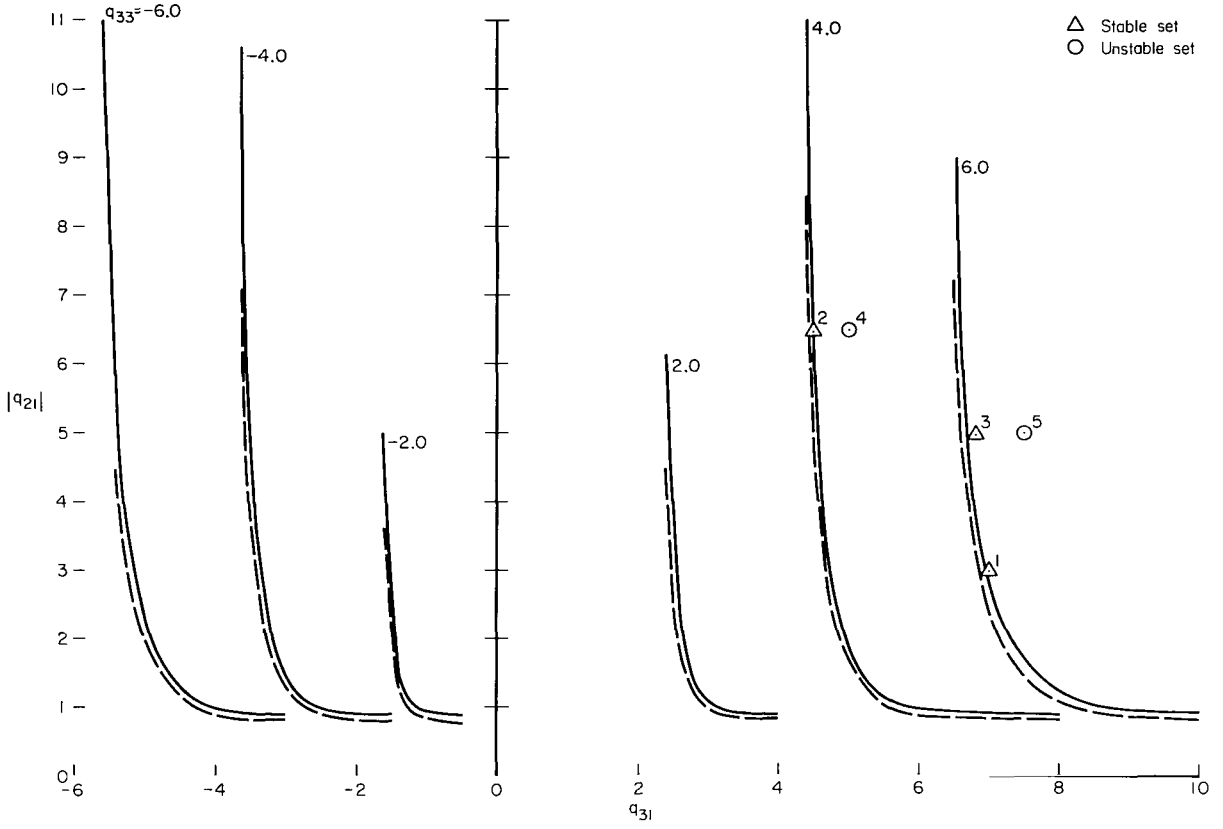

Figure 11.- Steady-state gain requirements - constant processor - trackers 1,2.

lines of constant q_{33} indicate the minimum q_{21} necessary to satisfy the drift rate specification. The dotted lines of constant q_{33} indicate the minimum q_{21} required to satisfy the pointing specification. The acceptable q_{21} for a given q_{31} lies above the constant q_{33} curve. The diagram shows that the sets of constants which satisfy the drift rate specification also satisfy the pointing accuracy specification. The symbols Δ and o in figure 11 represent sets of constants that satisfy the steady-state requirements and will be discussed in more detail in the following section.

Stability.- Stability of the system is determined for sets of constants that satisfy the steady-state requirements. System stability was investigated for the sets of constants given in table IV(b). As indicated in the table, sets 1, 2, and 3 provide stable operation of the system whereas sets 4 and 5 provide an unstable system over the range of parameters investigated ($-60^\circ \leq \gamma_1,\gamma_2 \leq +60^\circ$ and $1.11\times10^{-5} \leq N_2,N_3 \leq 1$). The degree of stability for

sets 1 and 2 is indicated by the parameter plane diagram of figure 10 where the plotted points represent the solution for the worst case. The sets of constants are also shown on figure 11 with an indication of the system stability. The Δ and o represent, respectively, a stable set and an unstable set. The superscript indicates the particular set of constants.

SIMULATION

The attitude control system was simulated on the analog computer to evaluate the performance of the system using each of the processors. The characteristics of the satellite and the control system are given in appendix D. Also, the star tracker gimbal angles and the characteristics for each processor are included in the appendix.

The purpose of the simulation was twofold. First, it was desired to validate the results of the stability analysis obtained from the digital computer. Second, it was desired to compare the performance of the system with the different processors. The simulation included the saturation type nonlinearity introduced by the motor but excluded the gyroscopic coupling torques due to motor rotation. The geometry transformation was described by the linearized equations (N matrix).

Ideal Processor

The system using the ideal processor to derive the attitude control signals was simulated on the analog computer. The system was designed so that the linear damping and natural frequency are, respectively, $\zeta \cong 0.7$ and $\omega_N \cong 1.2$. From the parameter plane (fig. 5), the variable parameters are as follows:

$$B1 = \frac{1}{\tau_2} = 2.0$$

$$B2 = N_i K = 14.32 \quad \text{where} \quad (N_i = 1)$$

As is to be expected from the relation in figure 6, the system then provides the desired steady-state performance for external torques less than 4750 dyne-cm.

The transient response of the system with the ideal processor is given in figure 12. The attitude error about each control channel is plotted twice so that the system response can be observed not only for large deviations but also for small deviations in the region near equilibrium. The figure shows that the control channels give identical responses to initial errors in position and are decoupled.

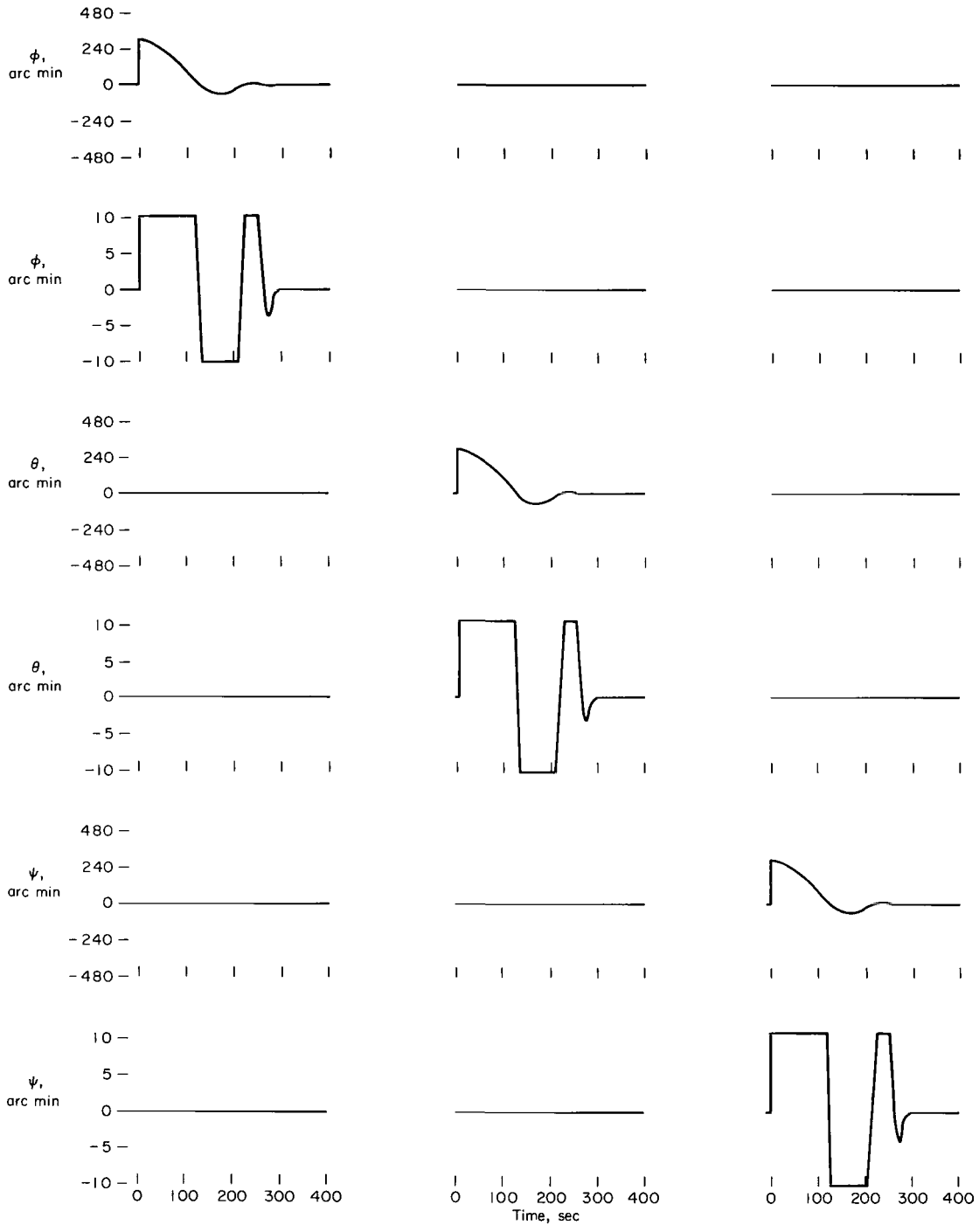

Figure 12.- Transient response of system using the ideal processor.

Partial Processor

The system using the partial processor was designed so that it exhibited the desired performance over the complete range of operating conditions. The minimum linear loop gain ($B2_{min}$) is chosen so that the desired steady-state performance is achieved for external torques less than or equal to 2000 dyne-cm (fig. 6); thus, $B2_{min} = 5.96$. From equation (37), $B2_{max} = 34.4$ for $|\gamma_1-\gamma_3| = 80^\circ$ which corresponds to a restricted region ($\Delta\gamma_R$) of 10°. The compensator time constant ($B1 = 1/\tau_2$) is chosen so that satisfactory performance is achieved over the complete range of B2. If B1 = 1.25, the damping ratio of the system varies from $\zeta \cong 0.25$ to $\zeta \cong 0.70$ as observed from the parameter plane (fig. 5).

The transient response of the system is indicated in appendix D (figures 13, 14, and 15). The response of the system to initial attitude errors of 5° about all control axes is shown in figure 13 when the loop gain is minimum (B2 = 5.96) and in figure 14 when the loop gain is maximum (B2 = 34.4). The difference between the two response curves is negligible because the linear range of the saturation type nonlinearity is so small that it functions like a relay; thus, the system functions in the nonlinear region most of the time.

The coupling between control channels is observed by comparing the three transient response runs displayed in figure 15. Each run shows the response of the system to an initial attitude error of 5° about a single control axis. Comparison of the runs indicates that pitch and yaw motion is coupled into the roll channel. Also, the pitch and yaw channels are observed to be independent.

Constant Processor

The system using the constant processor for tracker pair 1,3 and tracker pair 1,2 was also simulated. For a given set of constants, the gimbal angles were chosen in each case so that the system was operating under the most severe conditions.

The transient response of the system using the constant processor for tracker pair 1,3 is given in appendix D (figs. 16 and 17). The constants for the processor are $r_{23} = -4.25$, $|r_{31}| = 2.0$, and $|r_{33}| = 3.5$. Figure 16 shows runs in which an initial attitude error is imposed about a single control axis. The run on the left of the figure shows that roll motion is not coupled into pitch and yaw whereas the remaining two runs show that pitch and yaw motions are coupled into the other two channels. Figure 17 shows the response of the system when an initial attitude error is imposed simultaneously on all three control channels.

The response of the system using the constant processor for tracker pair 1,2 is given in appendix D (figs. 18 and 19). The response in both figures

is for the same set of constants ($|q_{21}| = 3.0$, $q_{31} = \begin{matrix}+7.0\\-6.0\end{matrix}$, and $q_{33} = \begin{matrix}+6.0\\-7.0\end{matrix}$) but for different gimbal angle values. Figure 18 shows the behavior of the system for gimbal angle values that provide the most unsatisfactory response. The yaw channel response clearly indicates that the coupling term dominates until the attitude error from the pitch channel sufficiently decreases. Figure 19 shows the behavior of the system for gimbal angle values that provide significantly improved response.

CONCLUSIONS

Three methods of processing star tracker information to derive attitude control signals have been developed. They are: (1) ideal processor, (2) partial processor, and (3) constant processor. The system using each of the processors exhibits acceptable transient and steady-state performance. Also, each of the processors is simple enough to be mechanized on board current spacecraft.

The star trackers are used in pairs to estimate the attitude errors of the satellite via the processors. The simplest form of the processors is obtained when the paired trackers are mounted to the vehicle so that their outer gimbal axes are parallel and when two inner and one outer gimbal error signals are used to derive the attitude control signals. The stability of the system is then independent of the inner gimbal angles of the star trackers.

An easily applied criterion for selecting stars (by ground operation) to avoid the indeterminant condition exists if the star trackers are used as suggested. The indeterminant condition implies that the attitude of the vehicle is unobservable; that is, the gimbal error signals being used to estimate the attitude errors are dependent. The condition occurs when the plane formed by the optical axes of the paired trackers contains the outer gimbal axes of the trackers. A region of restricted operation is established in the neighborhood of the indeterminant condition to insure that desired performance is maintained.

The ideal processor is the most complex of the three processors from the point of view of implementation because such trigonometric functions as the sine and cosine of the difference of gimbal angles and the tangent of gimbal angles must be mechanized. However, the control signals derived from this processor are independent and therefore provide a well-behaved system. The desired system performance is achieved over a commanded gimbal range that is limited only by the physical nature of the star tracker.

The partial processor is much simpler to mechanize than the ideal processor. Only the simple trigonometric functions such as the sine and cosine are mechanized with resolvers. The processor provides two control signals that are independent. Also, the required performance of the system is achieved over a commanded gimbal range that is again limited only by the physical nature of the star tracker.

Errors in mechanization of the partial processor have a negligible effect on the stability and performance of the system. To avoid problems due to errors in mechanization, it is only necessary to insure that the errors do not allow the system to operate in the region of restricted operation. Therefore, the restricted region must be increased by an amount equivalent to the error in mechanization.

The constant processor is the simplest of the three processors. Only amplifiers, potentiometers, and relays are required to mechanize terms that are constant in magnitude but vary in sign as a function of the outer gimbal angles. Performance of the system using the constant processor is acceptable over a gimbal angle range of $\pm 60^{\circ}$.

Ames Research Center
National Aeronautics and Space Administration
Moffett Field, Calif., 94035, Nov. 29, 1967
125-19-03-06-00-21

APPENDIX A

DERIVATION OF EQUATIONS RELATING THE MOTION OF THE TRACKERS AND VEHICLE

The relationship between the motion of the trackers and the motion of the vehicle is derived in this appendix. The relationship is obtained by expressing the motions as angular velocities and exploiting the simple transformation properties of angular velocity vectors.

Assuming that the tracker tracks its star without error, then the angular velocity of the vehicle in inertial space is the same as its velocity relative to the trackers. The inertial velocity can be expressed in terms of components along orthonormal axes fixed in the vehicle as $\omega_{1v}1^v + \omega_{2v}2^v + \omega_{3v}3^v$. The parameters of the tracker are needed to express the velocity of the vehicle relative to the tracker.

The sketch on the right of figure 2 shows the angles associated with tracker 1. These angles, with appropriate subscripts, are also associated with the other trackers. Each angle α relates a "line of sight" coordinate system $(l) = (1^l, 2^l, 3^l)$ to a coordinate system $(t) = (1^t, 2^t, 3^t)$ fixed to the tracker in such a way that $1^l = 1^t$. The (t) coordinates are related to a $(y) = (1^y, 2^y, 3^y)$ coordinate system by β so that $2^t = 2^y$. Similarly, (y) is related to an $(x) = (1^x, 2^x, 3^x)$ coordinate system by γ so that $3^y = 3^x$. The angles are positive when generated by right-hand rotations about their generating axes. Whereas the (l), (t), and (y) coordinates and their angles α, β, and γ move as the vehicle moves, the (x) coordinate is fixed to the vehicle in a way that varies from tracker to tracker. The (x) coordinate of each of the four trackers amounts to a permutation of the vehicle's coordinate system (v): thus (x) = P(v), where

$$\left.\begin{aligned} P_1 &= \begin{pmatrix} 0 & 1 & 0 \\ 0 & 0 & 1 \\ 1 & 0 & 0 \end{pmatrix}; \quad P_2 = \begin{pmatrix} 0 & -1 & 0 \\ 0 & 0 & -1 \\ 1 & 0 & 0 \end{pmatrix}; \\ P_3 &= \begin{pmatrix} 0 & 0 & 1 \\ 0 & -1 & 0 \\ 1 & 0 & 0 \end{pmatrix}; \quad P_4 = \begin{pmatrix} 0 & 0 & -1 \\ -1 & 0 & 0 \\ 0 & 1 & 0 \end{pmatrix} \end{aligned}\right\} \qquad (A1)$$

The inertial angular velocity of the vehicle in (x) coordinates is given as $\omega_{1x}1^x + \omega_{2x}2^x + \omega_{3x}3^x$. The fundamental relationship which states that this velocity is equal to the velocity relative to the tracker can be expressed in the form

$$\omega_{1x}1^x + \omega_{2x}2^x + \omega_{3x}3^x = \dot{\alpha}1^t + \dot{\beta}2^y + \dot{\gamma}3^x \tag{A2}$$

The following equations are obtained from the definitions of the coordinate systems:

$$\begin{pmatrix} 1^x \\ 2^x \\ 3^x \end{pmatrix} = \begin{pmatrix} c\gamma & s\gamma & 0 \\ -s\gamma & c\gamma & 0 \\ 0 & 0 & 1 \end{pmatrix} \begin{pmatrix} 1^y \\ 2^y \\ 3^y \end{pmatrix} \tag{A3}$$

$$\begin{pmatrix} 1^x \\ 2^x \\ 3^x \end{pmatrix} = \begin{pmatrix} c\gamma & s\gamma & 0 \\ -s\gamma & c\gamma & 0 \\ 0 & 0 & 1 \end{pmatrix} \begin{pmatrix} c\beta & 0 & -s\beta \\ 0 & 1 & 0 \\ s\beta & 0 & c\beta \end{pmatrix} \begin{pmatrix} 1^t \\ 2^t \\ 3^t \end{pmatrix} = \begin{pmatrix} c\gamma c\beta & s\gamma & -c\gamma s\beta \\ -s\gamma c\beta & c\gamma & s\gamma s\beta \\ s\beta & 0 & c\beta \end{pmatrix} \begin{pmatrix} 1^t \\ 2^t \\ 3^t \end{pmatrix} \tag{A4}$$

The 2^y equation and the 1^t equation are obtained by taking the inverse of equations (A3) and (A4) and are substituted into equation (A2) to give

$$\begin{pmatrix} \omega_{1x} \\ \omega_{2x} \\ \omega_{3x} \end{pmatrix} = \begin{pmatrix} c\gamma c\beta & s\gamma & 0 \\ -s\gamma c\beta & c\gamma & 0 \\ s\beta & 0 & 1 \end{pmatrix} \begin{pmatrix} \dot{\alpha} \\ \dot{\beta} \\ \dot{\gamma} \end{pmatrix} \tag{A5}$$

Inverting this transformation to solve for the tracker parameters gives

$$\begin{pmatrix} \dot{\alpha} \\ \dot{\beta} \\ \dot{\gamma} \end{pmatrix} = \frac{1}{c\beta} \begin{pmatrix} c\gamma & -s\gamma & 0 \\ s\gamma c\beta & c\gamma c\beta & 0 \\ -c\gamma s\beta & s\gamma s\beta & c\beta \end{pmatrix} \begin{pmatrix} \omega_{1x} \\ \omega_{2x} \\ \omega_{3x} \end{pmatrix} \tag{A6}$$

Equation (A6) holds for all the trackers, which differ from each other by the way they are mounted on the vehicle. The manner of mounting is

expressed by the permutation matrices in equation (A1). Postmultiplying the transformation matrix in equation (A6) by P_1, for example, relates the number 1 tracker parameters to the components of inertial angular velocity in vehicle coordinates:

$$\begin{pmatrix} \dot{\alpha}_1 \\ \dot{\beta}_1 \\ \dot{\gamma}_1 \end{pmatrix} = R \begin{pmatrix} \omega_{1v} \\ \omega_{2v} \\ \omega_{3v} \end{pmatrix} = \frac{1}{c\beta_1} \begin{pmatrix} 0 & c\gamma_1 & -s\gamma_1 \\ 0 & s\gamma_1 c\beta_1 & c\gamma_1 c\beta_1 \\ c\beta_1 & -c\gamma_1 s\beta_1 & s\gamma_1 s\beta_1 \end{pmatrix} \begin{pmatrix} \omega_{1v} \\ \omega_{2v} \\ \omega_{3v} \end{pmatrix} \tag{A7}$$

The rate transformation (R) for each of the trackers in figure 2 is obtained in a similar manner and is given in table I.

APPENDIX B

DERIVATION OF THE CHARACTERISTIC EQUATION FOR THE SYSTEM USING THE PARTIAL PROCESSOR WITH IMPERFECT MECHANIZATION

The equations describing the effect of errors in mechanization of the partial processor on the stability of the system are derived in this appendix. The errors are assumed small enough so that only the first-order terms are significant.

The partial processor for tracker pair 1,3 when perfectly mechanized is

$$M_P = \begin{bmatrix} 0 & 1 & 0 \\ d_{13}s\gamma_3 & 0 & -d_{13}c\gamma_1 \\ d_{13}c\gamma_3 & 0 & d_{13}s\gamma_1 \end{bmatrix} \tag{B1}$$

It is assumed that the constant terms are perfectly mechanized and that errors exist only in the gimbal angles γ_1 and γ_3. The errors result from either a misalinement of the resolvers used to mechanize the trigonometric functions or an inaccurate measurement of the gimbal angle. Gimbal angles with errors are represented by $\gamma_i + \Delta\gamma_i$. The partial processor with errors in mechanization is

$$M_{PE} = \begin{bmatrix} 0 & 1 & 0 \\ d_{13}s(\gamma_3+\Delta\gamma_3) & 0 & -d_{13}c(\gamma_1+\Delta\gamma_1) \\ d_{13}c(\gamma_3+\Delta\gamma_3) & 0 & d_{13}s(\gamma_1+\Delta\gamma_1) \end{bmatrix} \tag{B2}$$

The characteristic equation is

$$CE = DET(I+GM_{PE}N) = 0 \tag{B3}$$

where

$$G = \begin{bmatrix} g_1 & 0 & 0 \\ 0 & g_2 & 0 \\ 0 & 0 & g_3 \end{bmatrix}, \qquad g_i = \frac{N_i K(\tau_1 s + 1)}{s(\tau_2 s + 1)(\tau_m s + 1)} \tag{B4}$$

Define the following

$$\bar{G} = \begin{bmatrix} g & 0 & 0 \\ 0 & g & 0 \\ 0 & 0 & g \end{bmatrix}, \qquad g = \frac{K(\tau_1 s + 1)}{s(\tau_2 s + 1)(\tau_m s + 1)} \tag{B5}$$

$$D_F = \begin{bmatrix} N_1 & 0 & 0 \\ 0 & N_2 & 0 \\ 0 & 0 & N_3 \end{bmatrix} \tag{B6}$$

so that

$$B = D_F M_{PE} N = \begin{bmatrix} b_{11} & b_{12} & b_{13} \\ 0 & b_{22} & b_{23} \\ 0 & b_{32} & b_{33} \end{bmatrix} \tag{B7}$$

$$G = \bar{G} D_F$$

The characteristic equation is

$$CE = DET(I + \bar{G}B) = 0 \tag{B8}$$

or

$$CE = (1 + gN_1)(1 + B_T g + B_D g^2) = 0 \tag{B9}$$

where

$$B_T = b_{22} + b_{33} \tag{B10}$$

$$B_D = b_{22}b_{33} - b_{23}b_{32} \tag{B11}$$

The B matrix for the partial processor for tracker pair 1,3 is

$$B = \begin{bmatrix} N_1 & -N_1 c\gamma_1 t\beta_1 & N_1 s\gamma_1 t\beta_1 \\ 0 & \{N_2 d_{13}[s(\gamma_3+\Delta\gamma_3)s\gamma_1 + c(\gamma_1+\Delta\gamma_1)c\gamma_3]\} & \{N_2 d_{13}[s(\gamma_3+\Delta\gamma_3)c\gamma_1 - c(\gamma_1+\Delta\gamma_1)s\gamma_3]\} \\ 0 & \{N_3 d_{13}[c(\gamma_3+\Delta\gamma_3)s\gamma_1 - s(\gamma_1+\Delta\gamma_1)c\gamma_3]\} & \{N_3 d_{13}[c(\gamma_3+\Delta\gamma_3)c\gamma_1 + s(\gamma_1+\Delta\gamma_1)s\gamma_3]\} \end{bmatrix} \tag{B12}$$

If $\Delta\gamma_i$ is small enough so that the approximations $c\Delta\gamma_i = 1$ and $s\Delta\gamma_i = \Delta\gamma_i$ are valid, equation (B12) can be written as

$$B = \begin{bmatrix} N_1 & -N_1 c\gamma_1 t\beta_1 & N_1 s\gamma_1 t\beta_1 \\ 0 & \{N_2 d_{13}[c(\gamma_1-\gamma_3) + s\gamma_1 c\gamma_3(\Delta\gamma_3-\Delta\gamma_1)]\} & \{N_2 d_{13}[(c\gamma_3 c\gamma_1)\Delta\gamma_3 + (s\gamma_1 s\gamma_3)\Delta\gamma_1]\} \\ 0 & \{-N_3 d_{13}[(s\gamma_3 s\gamma_1)\Delta\gamma_3 + (c\gamma_1 c\gamma_3)\Delta\gamma_1]\} & \{N_3 d_{13}[c(\gamma_1-\gamma_3) - c\gamma_1 s\gamma_3(\Delta\gamma_3-\Delta\gamma_1)]\} \end{bmatrix} \quad (B13)$$

By using equation (B13), the parameter B_T (B10) can now be written as

$$B_T = (N_2 + N_3)d_{13}c(\gamma_1-\gamma_3) + d_{13}(N_2 s\gamma_1 c\gamma_3 - N_3 c\gamma_1 s\gamma_3)(\Delta\gamma_3-\Delta\gamma_1) \quad (B14)$$

Likewise, the parameter B_D (B11) can be written as follows.

$$B_D = N_2 N_3 d_{13}^2\{[c(\gamma_1-\gamma_3)]^2 + \delta[c(\gamma_1-\gamma_3)s(\gamma_1-\gamma_3)] - \delta^2[s\gamma_3 c\gamma_1 c\gamma_3 s\gamma_1]$$

$$+ [(c\gamma_3 c\gamma_1)\Delta\gamma_3 + (s\gamma_1 s\gamma_3)\Delta\gamma_1][(s\gamma_3 s\gamma_1)\Delta\gamma_3 + (c\gamma_3 c\gamma_1)\Delta\gamma_1]\} \quad (B15)$$

where

$$\delta = (\Delta\gamma_3-\Delta\gamma_1)$$

Equation (B15) reduces to the following when only the first-order error terms are considered significant.

$$B_D = N_2 N_3 d_{13}^2 c(\gamma_1-\gamma_3)\{c(\gamma_1-\gamma_3) + \delta[s(\gamma_1-\gamma_3)]\} \quad (B16)$$

Equations (B14) and (B16) define the parameters that are used in the characteristic equation (B9) to determine the effect of errors in mechanization on the stability of the system.

APPENDIX C

DETERMINATION OF STEADY-STATE PERFORMANCE FOR SYSTEM USING THE CONSTANT PROCESSOR

The equations describing the steady-state performance of the system using the constant processor are derived in this appendix. A block diagram of the system with all input parameters indicated is given by sketch (h)

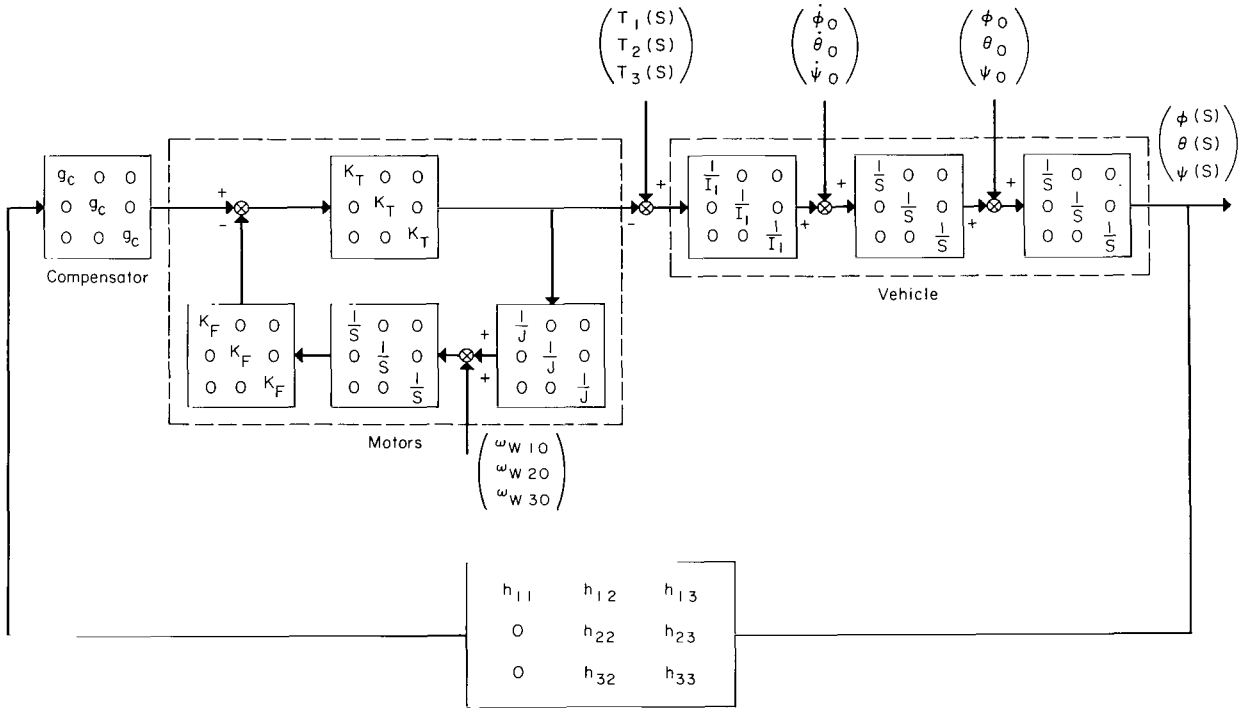

Sketch (h)

where

$$H = h_{ij} = M_c N \tag{C1}$$

$$g_c = \frac{K_c(\tau_1 s + 1)}{\tau_2 s + 1} \tag{C2}$$

Sketch (h) can be reduced to sketch (i)

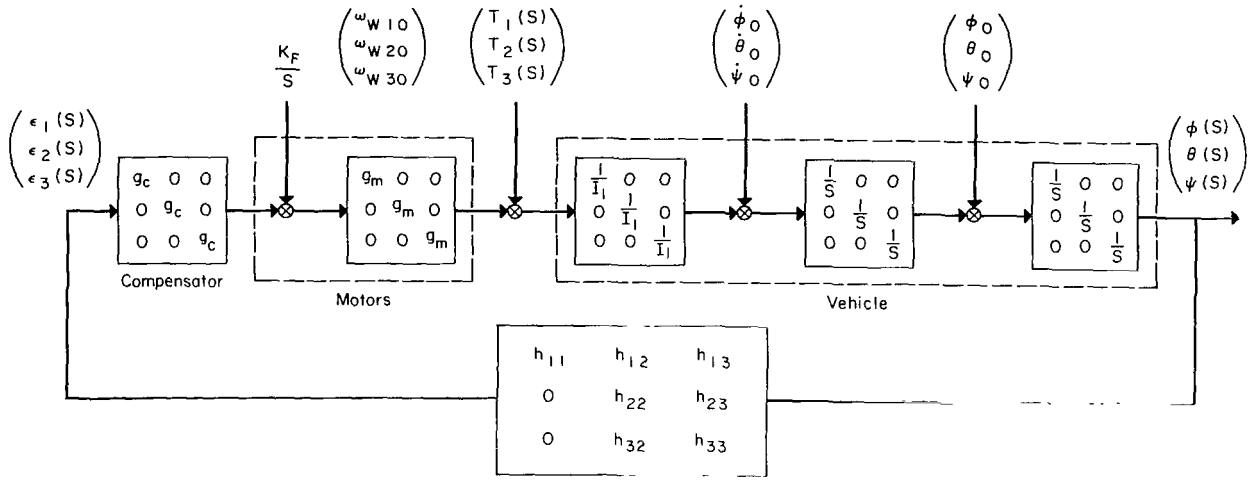

Sketch (i)

where

$$g_m = \frac{K_m s}{\tau_m s + 1} \tag{C3}$$

$$\frac{1}{\tau_m} = \frac{K_T K_F}{J}, \qquad K_m = \frac{J}{K_F} \tag{C4}$$

$$K = \frac{K_c K_m}{I_1} \tag{C5}$$

The steady-state performance is determined by writing the output parameters as a function of the input parameters and using the final value theorem; that is,

$$\begin{bmatrix} \varphi_{ss} \\ \theta_{ss} \\ \psi_{ss} \end{bmatrix} = \underset{s \to 0}{\text{Limit}}\ s \begin{bmatrix} \varphi(s) \\ \theta(s) \\ \psi(s) \end{bmatrix} = \underset{s \to 0}{\text{Limit}}\ sf \left(\begin{bmatrix} \dot{\varphi}_0 \\ \dot{\theta}_0 \\ \dot{\psi}_0 \end{bmatrix}, \begin{bmatrix} \omega_{w10} \\ \omega_{w20} \\ \omega_{w30} \end{bmatrix}, \begin{bmatrix} T_1(s) \\ T_2(s) \\ T_3(s) \end{bmatrix} \right) \tag{C6}$$

where the "ss" subscript indicates steady state.

The steady-state errors are determined as follows. The steady-state position error caused by an initial angular velocity of the vehicle and an initial angular velocity of the motor is

$$\begin{bmatrix} \varphi_{ss} \\ \theta_{ss} \\ \psi_{ss} \end{bmatrix} = W \begin{bmatrix} h_{1o} \\ h_{2o} \\ h_{3o} \end{bmatrix} \tag{C7}$$

where

$$W = \begin{bmatrix} \frac{1}{h_{11}K} & \left[\frac{h_{13}h_{32}-h_{12}h_{33}}{h_{11}KH_D}\right] & \left[\frac{h_{12}h_{23}-h_{13}h_{22}}{h_{11}KH_D}\right] \\ 0 & \left(\frac{h_{33}}{H_DK}\right) & \left(-\frac{h_{23}}{H_DK}\right) \\ 0 & \left(-\frac{h_{32}}{H_DK}\right) & \left(\frac{h_{22}}{H_DK}\right) \end{bmatrix} \tag{C8}$$

$$\begin{bmatrix} h_{1o} \\ h_{2o} \\ h_{3o} \end{bmatrix} = \begin{bmatrix} \dot{\varphi}_o - \frac{J}{I_1}\omega_{w1o} \\ \dot{\theta}_o - \frac{J}{I_1}\omega_{w2o} \\ \dot{\psi}_o - \frac{J}{I_1}\omega_{w3o} \end{bmatrix} \tag{C9}$$

H_D = determinant of H

The velocity error for a constant external torque about all three axes $[T_i(s) = t_i/s]$ is

$$\begin{bmatrix} \dot{\varphi}_{ss} \\ \dot{\theta}_{ss} \\ \dot{\psi}_{ss} \end{bmatrix} = \frac{1}{I_1} W \begin{bmatrix} t_1 \\ t_2 \\ t_3 \end{bmatrix} \tag{C10}$$

The steady-state pointing error and drift rate error are defined, respectively, by equations (C9) and (C10).

$$\text{Pointing error} = (\theta_{ss}^2 + \psi_{ss}^2)^{1/2} \leq PE \tag{C11}$$

$$\text{Drift rate error} = (\dot{\theta}_{ss}^2 + \dot{\psi}_{ss}^2)^{1/2} \leq DR \tag{C12}$$

where PE and DR are, respectively, the maximum allowable pointing error and the maximum allowable drift rate error. Use of equations (C7) and (C10) allows equations (C11) and (C12) to be written as follows:

$$\frac{1}{H_D K}\left[(h_{33}h_{20} - h_{23}h_{30})^2 + (-h_{32}h_{20} + h_{22}h_{30})^2\right]^{1/2} \leq PE \qquad (C13)$$

$$\frac{1}{H_D K}\left[\left(h_{33}\frac{t_2}{I_1} - h_{23}\frac{t_3}{I_1}\right)^2 + \left(-h_{32}\frac{t_2}{I_1} + h_{22}\frac{t_3}{I_1}\right)^2\right]^{1/2} \leq DR \qquad (C14)$$

The system will perform as required in steady state if the inequalities of (C13) and (C14) are satisfied. The equations are general since the constant processor for a particular tracker pair defines the H matrix. The steady-state performance of the system using the constant processor is now determined for the following two specific cases. They are: (1) tracker pair 1,3 and (2) tracker pair 1,2.

Tracker Pair 1,3

The H matrix for tracker pair 1,3 is

$$H = M_C N = \begin{bmatrix} 1 & (r_{11}s\gamma_1 - c\gamma_1 t\beta_1 - r_{13}c\gamma_3) & (r_{11}c\gamma_1 + s\gamma_1 t\beta_1 + r_{13}s\gamma_3) \\ 0 & (r_{21}s\gamma_1 - r_{23}c\gamma_3) & (r_{21}c\gamma_1 + r_{23}s\gamma_3) \\ 0 & (r_{31}s\gamma_1 - r_{33}c\gamma_3) & (r_{31}c\gamma_1 + r_{33}s\gamma_3) \end{bmatrix} \qquad (C15)$$

and

$$H_D = (r_{21}r_{33} - r_{23}r_{31})c(\gamma_1 - \gamma_3) \qquad (C16)$$

With $r_{21} = 0$ and equations (C15) and (C16), the pointing error equation (C13) becomes

$$\frac{\sqrt{[r_{31}^2 + r_{33}^2 - 2r_{31}r_{33}s(\gamma_1 - \gamma_3)]h_{20}^2 - \{2r_{23}[r_{33} - r_{31}s(\gamma_1 - \gamma_3)]\}h_{20}h_{30} + r_{23}^2 h_{30}^2}}{K[-r_{23}r_{31}c(\gamma_1 - \gamma_3)]} \leq PE \qquad (C17)$$

and must be evaluated at the most severe conditions. If it is assumed that $\Delta\gamma_R = 10^o$ and $|h_{20}| = |h_{30}|$, (C17) is evaluated at the following conditions.

$$\gamma_1-\gamma_3 = +80^o \qquad r_{21} = 0$$
$$h_{20} = -h_{30} \qquad r_{31} > 0 \qquad (C18)$$
$$r_{23} < 0 \qquad r_{33} < 0$$

In order to determine acceptable sets of constants, (C17) is written as a quadratic in r_{23} as indicated by

$$\{h_{30}^2 - [(PE)Kr_{31}c(\gamma_1-\gamma_3)]^2\}r_{23}^2 - \{2[r_{33}-r_{31}s(\gamma_1-\gamma_3)]h_{20}h_{30}\}r_{23}$$
$$+ [r_{31}^2 + r_{33}^2 - 2r_{31}r_{33}s(\gamma_1-\gamma_3)]h_{20}^2 \leq 0 \qquad (C19)$$

and is evaluated subject to the conditions listed in (C18). The allowable range of r_{23} for a given r_{31} and r_{33} that will satisfy the pointing accuracy specifications over the complete range of operating conditions can be determined.

The constants required to satisfy the drift rate specifications are determined in a like manner. In fact, from (C13) and (C14), the corresponding drift rate inequality can be written from (C19) and is

$$\{t_3^2 - [(DR)KI_1r_{31}c(\gamma_1-\gamma_3)]^2\}r_{23}^2 - \{2[r_{33}-r_{31}s(\gamma_1-\gamma_3)]t_2t_3\}r_{23}$$
$$+ [r_{31}^2 + r_{33}^2 - 2r_{31}r_{33}s(\gamma_1-\gamma_3)]t_2^2 \leq 0 \qquad (C20)$$

Equation (C20) is evaluated subject to the conditions listed in (C18) and $t_2 = -t_3$. The acceptable range of r_{23} for a given r_{31} and r_{33} that will satisfy the steady-state drift rate error for all operating conditions can then be calculated.

Tracker Pair 1,2

The H matrix for tracker pair 1,2 is

$$H = M_cN = \begin{bmatrix} 1 & (q_{11}s\gamma_1-c\gamma_1t\beta_1-q_{13}s\gamma_2) & (q_{11}c\gamma_1+s\gamma_1t\beta_1-q_{13}c\gamma_2) \\ 0 & q_{21}(s\gamma_1-s\gamma_2) & q_{21}(c\gamma_1-c\gamma_2) \\ 0 & (q_{31}s\gamma_1-q_{33}s\gamma_2) & (q_{31}c\gamma_1-q_{33}c\gamma_2) \end{bmatrix} \qquad (C21)$$

where

$$q_{21} = q_{23}$$

$$H_D = q_{21}(q_{31}-q_{33})s(\gamma_1-\gamma_2)$$

The elements of the matrix in equation (C21) can be substituted into equation (C13) to provide the following equation

$$([q_{31}^2 + q_{33}^2 - 2q_{31}q_{33}c(\gamma_1-\gamma_2)]h_{20}^2 - \{2q_{21}(q_{31}+q_{33})[1 - c(\gamma_1-\gamma_2)]\}h_{20}h_{30}$$

$$+ \{2q_{21}^2[1 - c(\gamma_1-\gamma_2)]\}h_{30}^2)^{1/2}[Kq_{21}(q_{31}-q_{33})s(\gamma_1-\gamma_2)]^{-1} \leq PE \qquad (C22)$$

The inequality of (C22) is written as a quadratic in q_{21} (C23) so that sets of constants can be determined that will satisfy the steady-state pointing accuracy.

$$\{[(PE)K(q_{31}-q_{33})s(\gamma_1-\gamma_2)]^2 - 2[1 - c(\gamma_1-\gamma_2)]h_{30}^2\}q_{21}^2$$

$$+(\{2(q_{31}+q_{33})[1 - c(\gamma_1-\gamma_2)]\}h_{20}h_{30})q_{21}$$

$$- [q_{31}^2 + q_{33}^2 - 2q_{31}q_{33}c(\gamma_1-\gamma_2)]h_{20}^2 \geq 0 \qquad (C23)$$

The most restricted range of q_{21} for a given q_{31} and q_{33} is determined if (C23) is evaluated at the most severe conditions.

As before, the inequality for drift rate error can be written directly from (C23) and is

$$\left\{[(DR)K(q_{31}-q_{33})s(\gamma_1-\gamma_2)]^2 - 2[1 - c(\gamma_1-\gamma_2)]\left(\frac{t_3}{I_1}\right)^2\right\}q_{21}^2$$

$$+\left(\{2(q_{31}+q_{33})[1 - c(\gamma_1-\gamma_2)]\}\frac{t_2}{I_1}\frac{t_3}{I_1}\right)q_{21}$$

$$- [q_{31}^2 + q_{33}^2 - 2q_{31}q_{33}c(\gamma_1-\gamma_2)]\left(\frac{t_2}{I_1}\right)^2 \geq 0 \qquad (C24)$$

Again the parameters are chosen so that the worse case is obtained; that is, it is necessary to choose the sign of t_2 and t_3 and the magnitude of $(\gamma_1-\gamma_2)$ that results in the most severe condition. The results of the calculations are plotted in figure 11.

APPENDIX D

CHARACTERISTICS OF THE SATELLITE

Vehicle characteristics

$I_1 = I_{ii} = 1952$ kg-m^2 (1440 slug-ft^2) $\quad i = 1, 2, 3$

$I_{ij} = 0$

Motor characteristics

Stall torque = $T_s = 0.0353$ N-m (5 in.-oz)

Time constant = $\tau_m = 76.8$ sec

$K_m = 0.1041$ N-m-sec (0.0768 ft-lb-sec)

Compensator characteristics

Ideal processor

$K_c = 268{,}000 \frac{1}{\text{radians}}$

$\tau_1 = 5.27$ sec

$\tau_2 = 0.527$ sec

Partial processor

$K_c = 268{,}000 \frac{1}{\text{radians}}$

$\tau_1 = 8.0$ sec

$\tau_2 = 0.8$ sec

Constant processor

$K_c = 268{,}000 \frac{1}{\text{radians}}$

$\tau_1 = 5.0$ sec

$\tau_2 = 0.5$ sec

Processor and geometry

Ideal processor

Unity feedback

Partial processor

$|d_{13}| = 2.4$

$\beta_1 = 30^\circ$

$\gamma_1 = 60^\circ$

Figure 13

$\gamma_1 - \gamma_3 = 80^\circ$ where $\gamma_3 = -20^\circ$

Figures 14 and 15

$\gamma_1 - \gamma_3 = 0^\circ$ where $\gamma_3 = 60^\circ$

Constant processor

Tracker pair 1,3 - figures 16 and 17

$r_{23} = -4.25$ $r_{31} = 2.0$ $r_{33} = -3.5$

$\gamma_1 = -35^\circ$ $\beta_1 = 30^\circ$ $\gamma_3 = -45^\circ$

Tracker pair 1,2

Figure 18

$q_{21} = q_{23} = 3.0$ $q_{31} = -6.0$ $q_{33} = -7.0$

$\gamma_1 = 60^\circ$ $\beta_1 = 30^\circ$ $\gamma_2 = -60^\circ$

Figure 19

$q_{21} = q_{23} = 3.0$ $q_{31} = 7.0$ $q_{33} = 6.0$

$\gamma_1 = -50^\circ$ $\beta_1 = 30^\circ$ $\gamma_2 = -60^\circ$

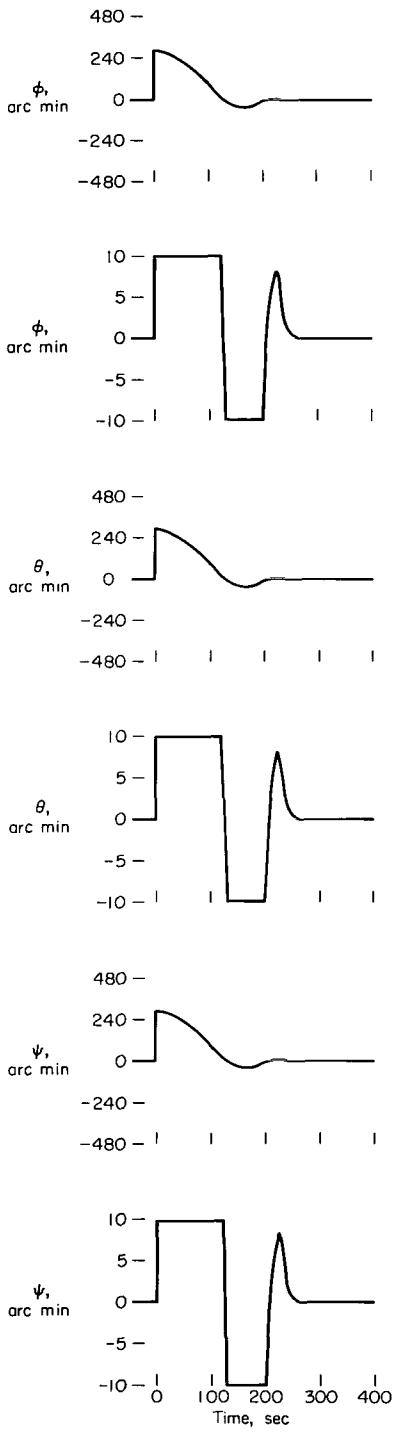

Figure 13.- Transient response of system using the partial processor - minimum loop gain.

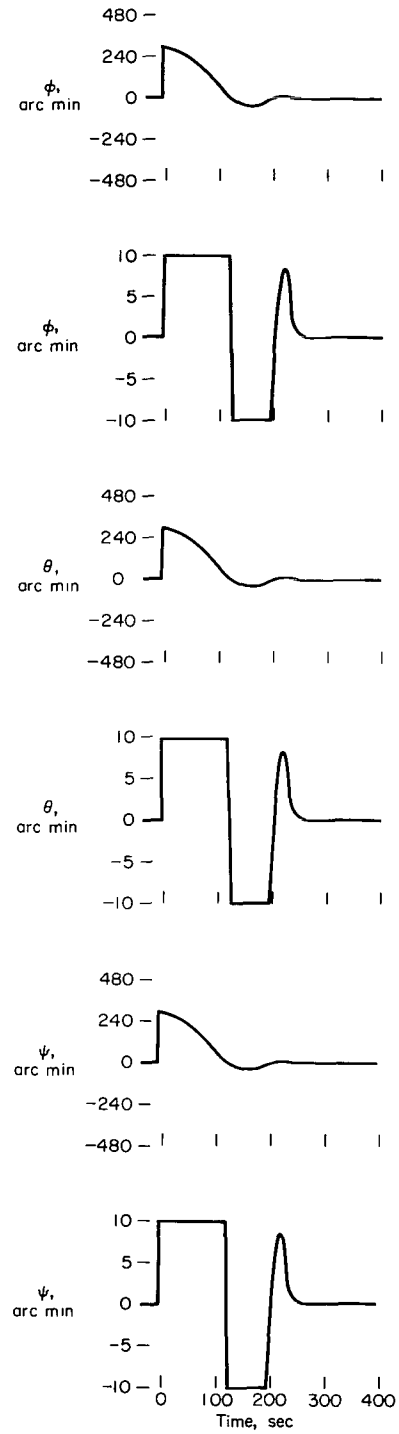

Figure 14.- Transient response of system using the partial processor - maximum loop gain.

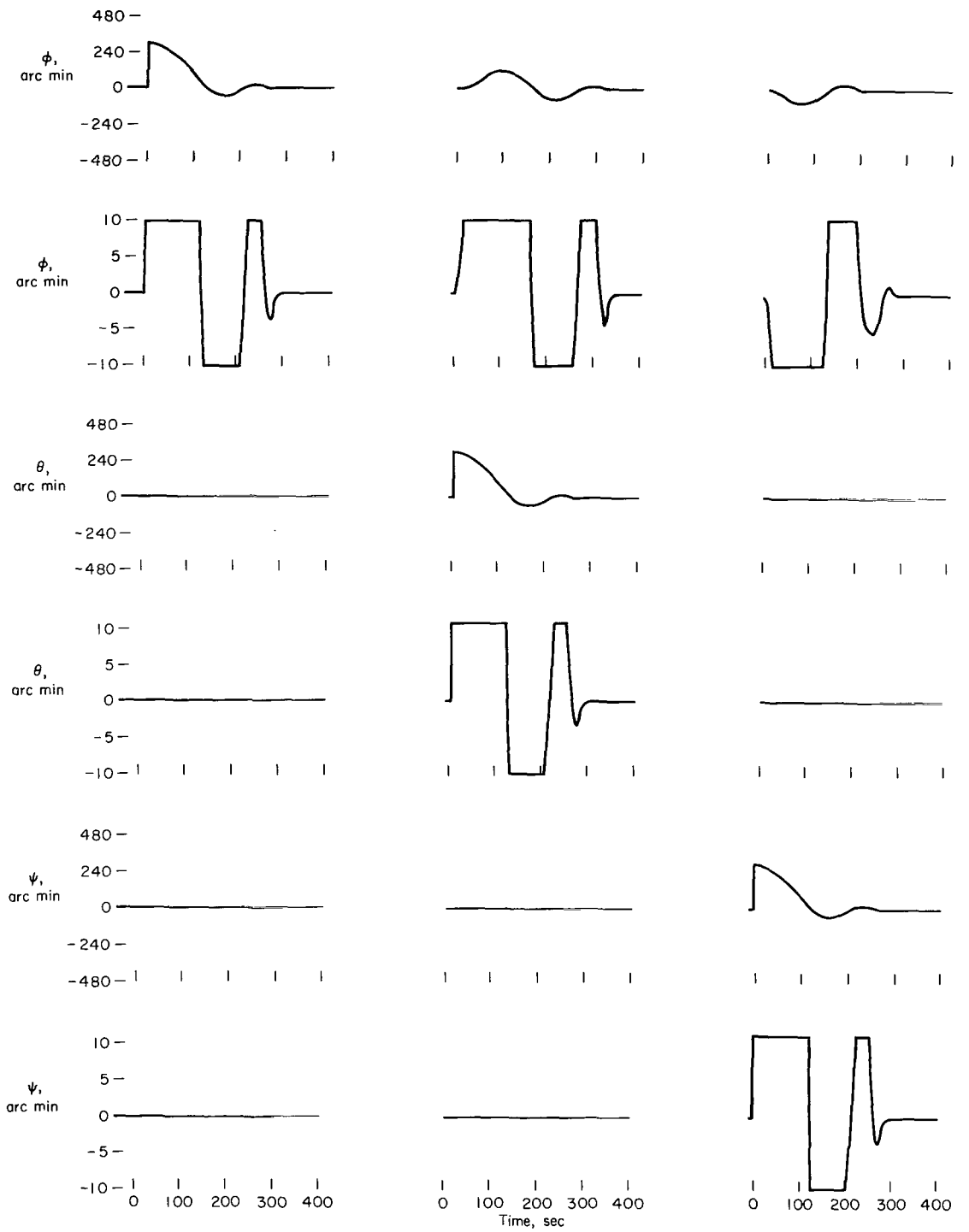

Figure 15.- Transient response of system using the partial processor - initial position error about single axis to show coupling.

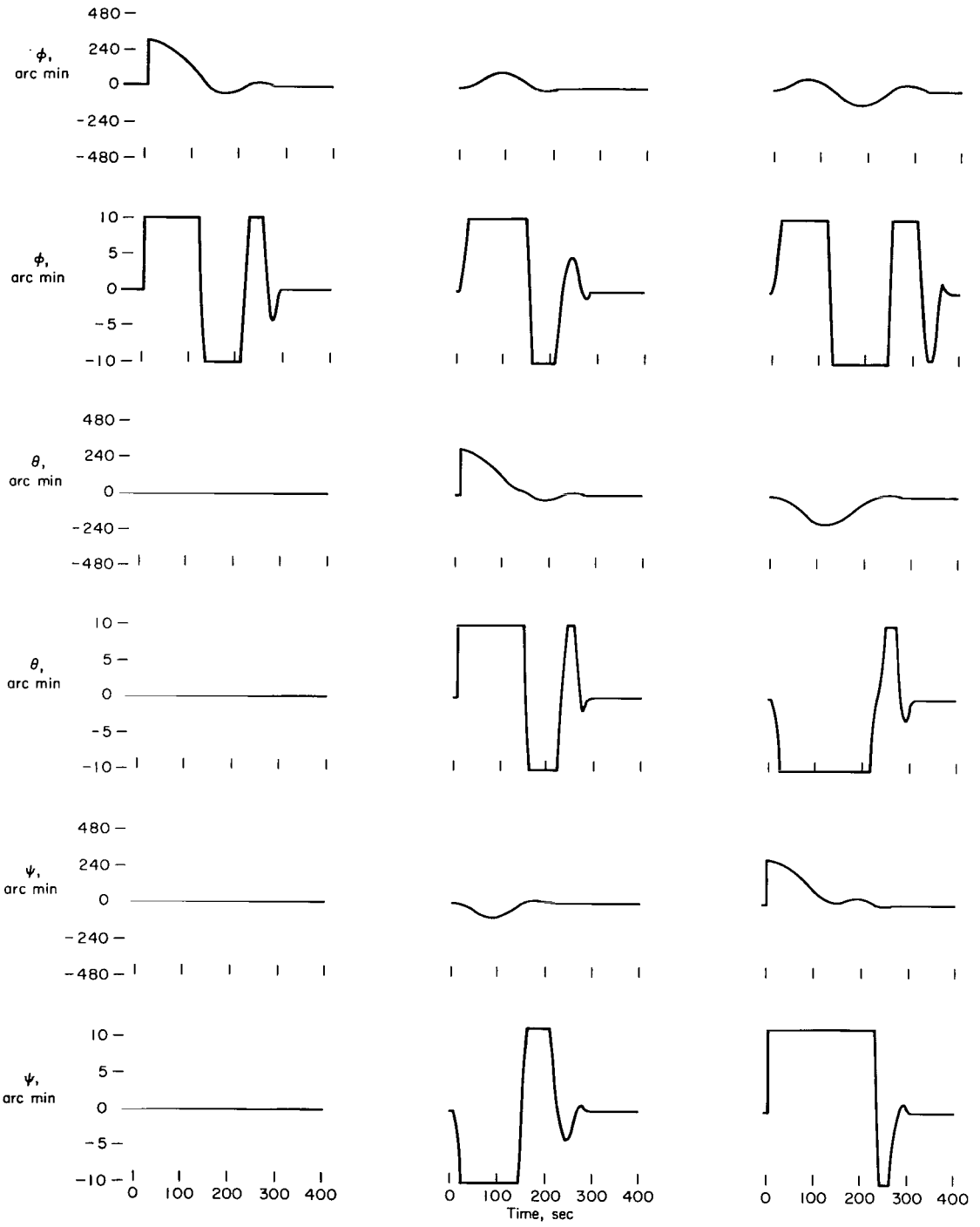

Figure 16.- Transient response of system using the constant processor for trackers 1,3 - initial position error about single axis to show coupling.

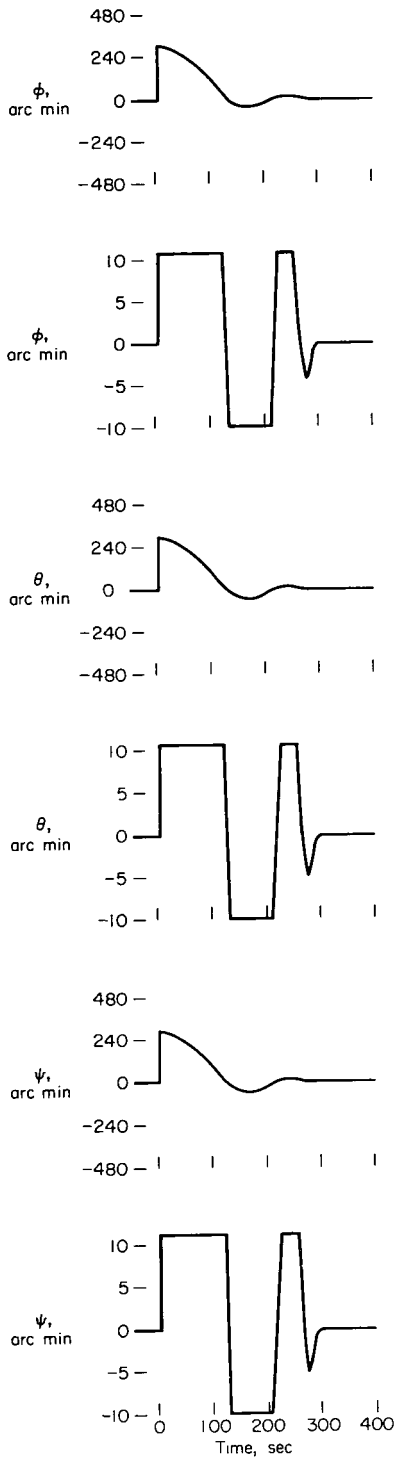

Figure 17.- Transient response of system using the constant processor for trackers 1,3 - initial position error about all three axes.

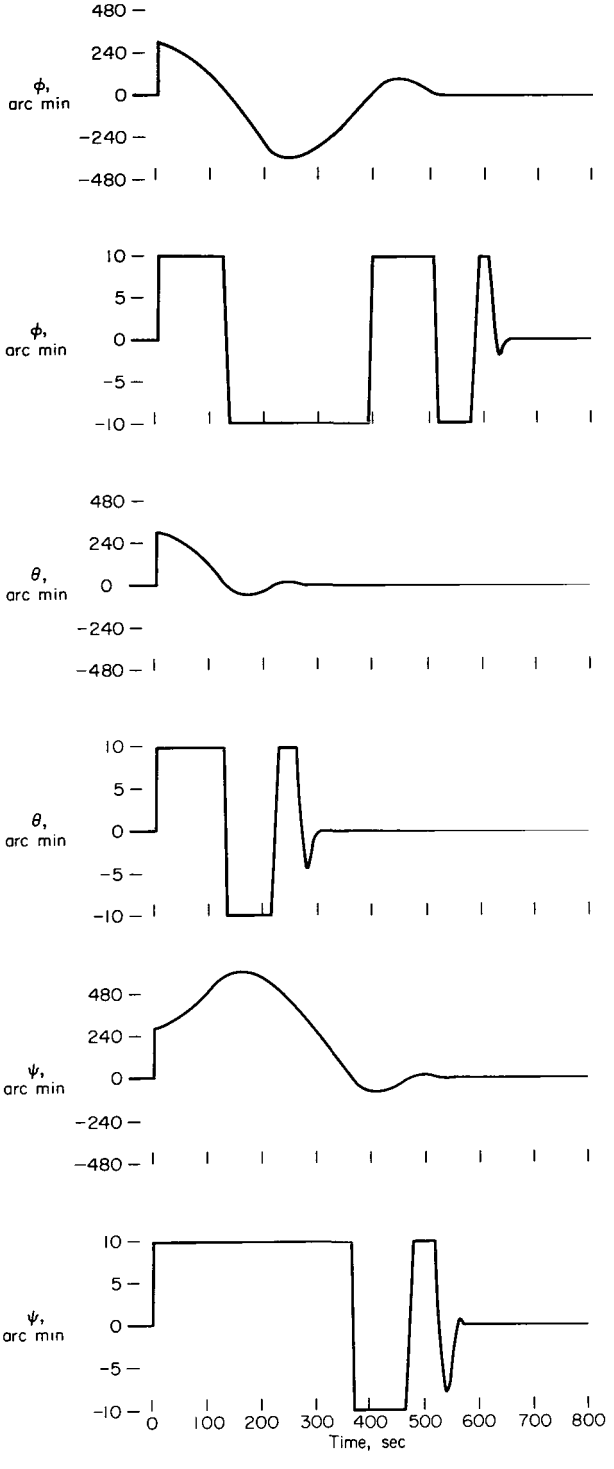

Figure 18.- Transient response of system using the constant processor for trackers 1,2 - worst case gimbal angles.

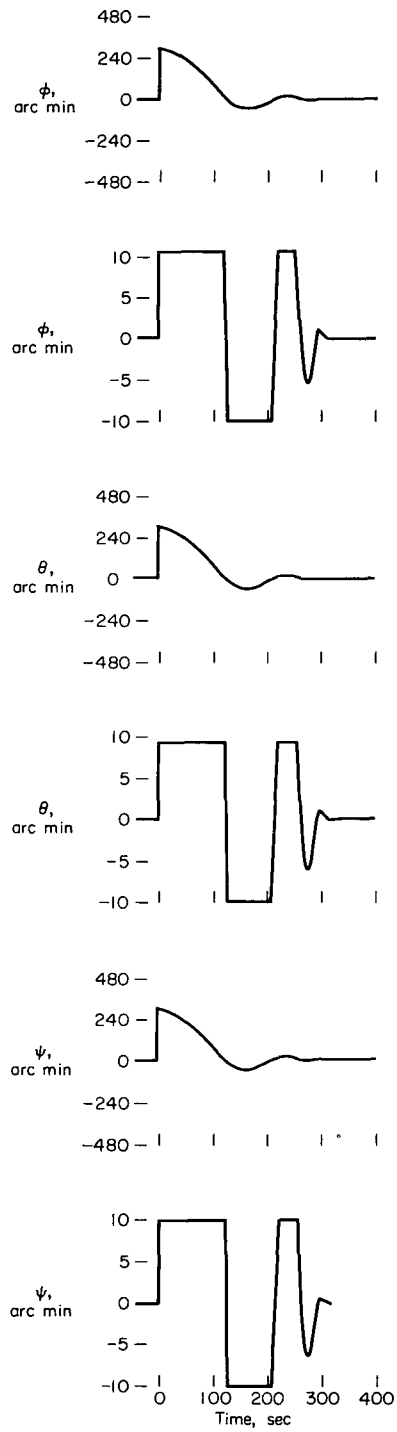

Figure 19.- Transient response of system using the constant processor for trackers 1,2 - arbitrary gimbal angles.

REFERENCES

1. Meyer, George: On the Use of Euler's Theorem on Rotations for the Synthesis of Attitude Control Systems. NASA TN D-3643, 1966.

2. Zetkov, George; and Fleisig, Ross: Dynamic Analysis of OAO Spacecraft Motion by Analog-Digital Simulation. 1962 IRE International Convention Record. Pt. 5 - Aerospace and Navigational Electronics; Military Electronics; Radio Frequency Interference; Space Electronics and Telemetry, vol. 10, pp. 282-296.

3. Kligerman, J. L.: A Stability Criteria for an Artificial Earth Satellite. Presented at the Tenth Annual East Coast Conference on Aerospace and Navigational Electronics, Oct. 21-23, 1963, pp. 1.5.5-1 - 1.5.5-10.

4. Thaler, G. J.; and Brown, R. G.: Analysis and Design of Feedback Control Systems. McGraw-Hill Book Co., Inc., 1960.

5. Siljak, D. D.: Feedback Control Systems in the Parameter Plane - Parts I, II, and III. IEEE Trans. Application and Industry, vol. 83, no. 75, pp. 449-473, Nov. 1964.

TABLE I.- TRANSFORMATION R RELATING THE STAR TRACKER GIMBAL RATES AND THE VEHICLE INERTIAL RATES

Tracker	[ ] = [R][ ]
1	$\begin{bmatrix} \dot{\alpha}_1 \\ \dot{\beta}_1 \\ \dot{\gamma}_1 \end{bmatrix} = \begin{bmatrix} 0 & c\gamma_1/c\beta_1 & -s\gamma_1/c\beta_1 \\ 0 & s\gamma_1 & c\gamma_1 \\ 1 & -c\gamma_1 t\beta_1 & s\gamma_1 t\beta_1 \end{bmatrix} \begin{bmatrix} \omega_1 \\ \omega_2 \\ \omega_3 \end{bmatrix}$
2	$\begin{bmatrix} \dot{\alpha}_2 \\ \dot{\beta}_2 \\ \dot{\gamma}_2 \end{bmatrix} = \begin{bmatrix} 0 & -c\gamma_2/c\beta_2 & s\gamma_2/c\beta_2 \\ 0 & -s\gamma_2 & -c\gamma_2 \\ 1 & c\gamma_2 t\beta_2 & -s\gamma_2 t\beta_2 \end{bmatrix} \begin{bmatrix} \omega_1 \\ \omega_2 \\ \omega_3 \end{bmatrix}$
3	$\begin{bmatrix} \dot{\alpha}_3 \\ \dot{\beta}_3 \\ \dot{\gamma}_3 \end{bmatrix} = \begin{bmatrix} 0 & s\gamma_3/c\beta_3 & c\gamma_3/c\beta_3 \\ 0 & -c\gamma_3 & s\gamma_3 \\ 1 & -s\gamma_3 t\beta_3 & -c\gamma_3 t\beta_3 \end{bmatrix} \begin{bmatrix} \omega_1 \\ \omega_2 \\ \omega_3 \end{bmatrix}$
4	$\begin{bmatrix} \dot{\alpha}_4 \\ \dot{\beta}_4 \\ \dot{\gamma}_4 \end{bmatrix} = \begin{bmatrix} s\gamma_4/c\beta_4 & 0 & -c\gamma_4/c\beta_4 \\ -c\gamma_4 & 0 & -s\gamma_4 \\ -s\gamma_4 t\beta_4 & 1 & c\gamma_4 t\beta_4 \end{bmatrix} \begin{bmatrix} \omega_1 \\ \omega_2 \\ \omega_3 \end{bmatrix}$

TABLE II.- TRANSFORMATIONS DESCRIBING THE GEOMETRY (N) AND THE PROCESSORS (M, M_p, M_c) FOR PAIRS OF TRACKERS

Tracker pair	[ ] = [N][ ]	[ ] = [M][ ]
1,2	$\begin{bmatrix}\Delta\beta_1\\ \Delta\gamma_1\\ \Delta\beta_2\end{bmatrix} = \begin{bmatrix}0 & s\gamma_1 & c\gamma_1\\ 1 & -c\gamma_1 t\beta_1 & s\gamma_1 t\beta_1\\ 0 & -s\gamma_2 & -c\gamma_2\end{bmatrix}\begin{bmatrix}\Delta\varphi\\ \Delta\theta\\ \Delta\psi\end{bmatrix}$	$\begin{bmatrix}\epsilon_\varphi\\ \epsilon_\theta\\ \epsilon_\psi\end{bmatrix} = \frac{1}{D_{12}}\begin{bmatrix}c(\gamma_1-\gamma_2)t\beta_1 & s(\gamma_1-\gamma_2) & t\beta_1\\ c\gamma_2 & 0 & c\gamma_1\\ -s\gamma_2 & 0 & -s\gamma_1\end{bmatrix}\begin{bmatrix}\Delta\beta_1\\ \Delta\gamma_1\\ \Delta\beta_2\end{bmatrix}$ $D_{12} = s(\gamma_1-\gamma_2)$
1,3	$\begin{bmatrix}\Delta\beta_1\\ \Delta\gamma_1\\ \Delta\beta_3\end{bmatrix} = \begin{bmatrix}0 & s\gamma_1 & c\gamma_1\\ 1 & -c\gamma_1 t\beta_1 & s\gamma_1 t\beta_1\\ 0 & -c\gamma_3 & s\gamma_3\end{bmatrix}\begin{bmatrix}\Delta\varphi\\ \Delta\theta\\ \Delta\psi\end{bmatrix}$	$\begin{bmatrix}\epsilon_\varphi\\ \epsilon_\theta\\ \epsilon_\psi\end{bmatrix} = \frac{1}{D_{13}}\begin{bmatrix}s(\gamma_3-\gamma_1)t\beta_1 & c(\gamma_1-\gamma_3) & -t\beta_1\\ s\gamma_3 & 0 & -c\gamma_1\\ c\gamma_3 & 0 & s\gamma_1\end{bmatrix}\begin{bmatrix}\Delta\beta_1\\ \Delta\gamma_1\\ \Delta\beta_3\end{bmatrix}$ $D_{13} = c(\gamma_1-\gamma_3)$
1,4	$\begin{bmatrix}\Delta\beta_1\\ \Delta\gamma_1\\ \Delta\beta_4\end{bmatrix} = \begin{bmatrix}0 & s\gamma_1 & c\gamma_1\\ 1 & -c\gamma_1 t\beta_1 & s\gamma_1 t\beta_1\\ -c\gamma_4 & 0 & -s\gamma_4\end{bmatrix}\begin{bmatrix}\Delta\varphi\\ \Delta\theta\\ \Delta\psi\end{bmatrix}$	$\begin{bmatrix}\epsilon_\varphi\\ \epsilon_\theta\\ \epsilon_\psi\end{bmatrix} = \frac{1}{D_{14}}\begin{bmatrix}c\gamma_1 t\beta_1 s\gamma_4 & s\gamma_1 s\gamma_4 & t\beta_1\\ s\gamma_4 - c\gamma_4 s\gamma_1 t\beta_1 & c\gamma_1 c\gamma_4 & c\gamma_1\\ -c\gamma_1 t\beta_1 c\gamma_4 & -s\gamma_1 c\gamma_4 & -s\gamma_1\end{bmatrix}\begin{bmatrix}\Delta\beta_1\\ \Delta\gamma_1\\ \Delta\beta_4\end{bmatrix}$ $D_{14} = s\gamma_1 s\gamma_4 - c\gamma_4 t\beta_1$
1,2	$\begin{bmatrix}\Delta\beta_1\\ \Delta\gamma_1\\ \Delta\gamma_2\end{bmatrix} = \begin{bmatrix}0 & s\gamma_1 & c\gamma_1\\ 1 & -c\gamma_1 t\beta_1 & s\gamma_1 t\beta_1\\ 1 & c\gamma_2 t\beta_2 & -s\gamma_2 t\beta_2\end{bmatrix}\begin{bmatrix}\Delta\varphi\\ \Delta\theta\\ \Delta\psi\end{bmatrix}$	$\begin{bmatrix}\epsilon_\varphi\\ \epsilon_\theta\\ \epsilon_\psi\end{bmatrix} = \frac{1}{F_{12}}\begin{bmatrix}-s(\gamma_1-\gamma_2)t\beta_1 t\beta_2 & c(\gamma_1-\gamma_2)t\beta_2 & t\beta_1\\ s\gamma_2 t\beta_2 + s\gamma_1 t\beta_1 & -c\gamma_1 & c\gamma_1\\ c\gamma_2 t\beta_2 + c\gamma_1 t\beta_1 & s\gamma_1 & -s\gamma_1\end{bmatrix}\begin{bmatrix}\Delta\beta_1\\ \Delta\gamma_1\\ \Delta\gamma_2\end{bmatrix}$ $F_{12} = t\beta_1 + c(\gamma_1-\gamma_2)t\beta_2$
Tracker pair	**[ ] = [M_p][ ]**	**[ ] = [M_c][ ]**
1,2	$\begin{bmatrix}\epsilon\varphi\\ \epsilon\theta\\ \epsilon\psi\end{bmatrix} = \begin{bmatrix}u_{11} & 1 & u_{13}\\ d_{12}c\gamma_2 & 0 & d_{12}c\gamma_1\\ -d_{12}s\gamma_2 & 0 & -d_{12}s\gamma_1\end{bmatrix}\begin{bmatrix}\Delta\beta_1\\ \Delta\gamma_1\\ \Delta\beta_2\end{bmatrix}$	$\begin{bmatrix}\epsilon_\varphi\\ \epsilon_\theta\\ \epsilon_\psi\end{bmatrix} = \begin{bmatrix}q_{11} & 1 & q_{13}\\ q_{21} & 0 & q_{23}\\ q_{31} & 0 & q_{33}\end{bmatrix}\begin{bmatrix}\Delta\beta_1\\ \Delta\gamma_1\\ \Delta\beta_2\end{bmatrix}$
1,3	$\begin{bmatrix}\epsilon\varphi\\ \epsilon\theta\\ \epsilon\psi\end{bmatrix} = \begin{bmatrix}v_{11} & 1 & v_{13}\\ d_{13}s\gamma_3 & 0 & -d_{13}c\gamma_1\\ d_{13}c\gamma_3 & 0 & d_{13}s\gamma_1\end{bmatrix}\begin{bmatrix}\Delta\beta_1\\ \Delta\gamma_1\\ \Delta\beta_3\end{bmatrix}$	$\begin{bmatrix}\epsilon_\varphi\\ \epsilon_\theta\\ \epsilon_\psi\end{bmatrix} = \begin{bmatrix}r_{11} & 1 & r_{13}\\ r_{21} & 0 & r_{23}\\ r_{31} & 0 & r_{33}\end{bmatrix}\begin{bmatrix}\Delta\beta_1\\ \Delta\gamma_1\\ \Delta\beta_3\end{bmatrix}$
1,4	No partial processor	No constant processor
1,2	No partial processor	No constant processor

TABLE III.- DATA REQUIRED FOR EVALUATING STEADY-STATE PERFORMANCE OF SYSTEM

PE = 1 arc min

DR = 15 arc sec for 50 min

$\dot{\theta}_o = \dot{\psi}_o = 0$

$|t_2| = |t_3|$

$|\omega_{wi}|_{max} = 1000$ rpm

$|\omega_{w2o}| = |\omega_{w3o}| = 0.4\ |\omega_{wi}|_{max}$

K = 14.32

$I_1 = 1952$ kg-m^2 (1440 slug-ft^2)

$|t_2| = |t_3| = 10^{-4}$ N-m (10^3 dyne-cm)

TABLE IV.- SETS OF CONSTANTS FOR THE CONSTANT PROCESSOR

(a) Tracker pair 1,3

Set	r_{21}	r_{23}	$\lvert r_{31} \rvert$	$\lvert r_{33} \rvert$	Stability
1	0	-4.25	2.0	3.5	Stable
2	0	-3.5	2.5	4.0	Stable
3	0	-4.0	2.0	3.0	Stable
4	0	-3.5	2.0	2.5	Unstable
5	0	-3.0	2.0	2.0	Unstable

(b) Tracker pair 1,2

Set	$\lvert q_{21} \rvert$	$\lvert q_{31} \rvert$	$\lvert q_{33} \rvert$	Stability
1	3.0	7.0 -6.0	6.0 -7.0	Stable
2	6.5	4.5 -4.0	4.0 -4.5	Stable
3	5.0	6.8 -6.0	6.0 -6.8	Stable
4	6.5	5.0 -4.0	4.0 -5.0	Unstable
5	5.0	7.5 -6.0	6.0 -7.5	Unstable

NASA-Langley, 1968 —— 21 A-2474

"The aeronautical and space activities of the United States shall be conducted so as to contribute . . . to the expansion of human knowledge of phenomena in the atmosphere and space. The Administration shall provide for the widest practicable and appropriate dissemination of information concerning its activities and the results thereof."

—NATIONAL AERONAUTICS AND SPACE ACT OF 1958

NASA SCIENTIFIC AND TECHNICAL PUBLICATIONS

TECHNICAL REPORTS: Scientific and technical information considered important, complete, and a lasting contribution to existing knowledge.

TECHNICAL NOTES: Information less broad in scope but nevertheless of importance as a contribution to existing knowledge.

TECHNICAL MEMORANDUMS: Information receiving limited distribution because of preliminary data, security classification, or other reasons.

CONTRACTOR REPORTS: Scientific and technical information generated under a NASA contract or grant and considered an important contribution to existing knowledge.

TECHNICAL TRANSLATIONS: Information published in a foreign language considered to merit NASA distribution in English.

SPECIAL PUBLICATIONS: Information derived from or of value to NASA activities. Publications include conference proceedings, monographs, data compilations, handbooks, sourcebooks, and special bibliographies.

TECHNOLOGY UTILIZATION PUBLICATIONS: Information on technology used by NASA that may be of particular interest in commercial and other non-aerospace applications. Publications include Tech Briefs, Technology Utilization Reports and Notes, and Technology Surveys.

Details on the availability of these publications may be obtained from:

SCIENTIFIC AND TECHNICAL INFORMATION DIVISION

NATIONAL AERONAUTICS AND SPACE ADMINISTRATION

Washington, D.C. 20546